ASC

ASTRO
SCIENCES
CENTER

109p.

N64-19566
CODE-1
NASA CR-53729

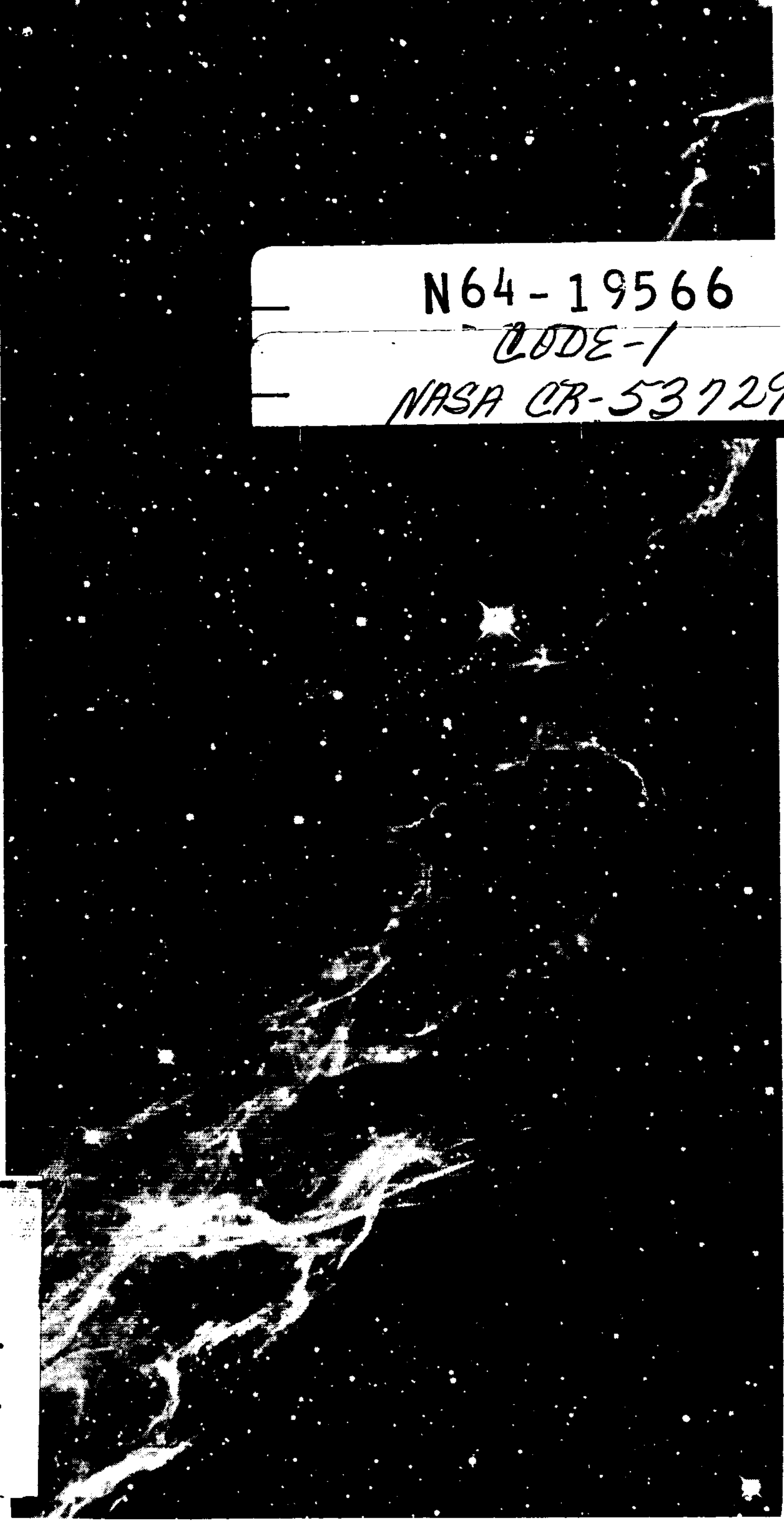

OTS PRICE

XEROX $ 9.10 ph

MICROFILM $ 3.47 mf.

Report No. M-3

A SURVEY OF MISSIONS TO THE ASTEROIDS

(NASA CR-53729; OTS: $9.10 ph, ~~$3.47 mf~~

Report No. M-3)

Title [A SURVEY OF MISSIONS TO THE ASTEROIDS

by

A. L. Friedlander and
R. S. Vickers

Astro Sciences Center
IIT RESEARCH INST~~ITUTE~~
Chicago, Ill~~inois~~

1252352

[8]

for

Lunar and Planetary Programs
National Aeronautics and Space Administration
Washington, D. C.

(NASA Contract ~~No.~~ NASr-65(06))

APPROVED:

L. Reiffel

L. Reiffel, Director

[1963] 109p refs

IIT RESEARCH INSTITUTE

ACKNOWLEDGEMENT

This task was coordinated by R. S. Vickers. The contributions, comments and criticisms of the ASC staff are gratefully acknowledged.

ABSTRACT

19566 A-24

A survey has been made of possible missions to the asteroid belt, and to asteroids whose orbits bring them in close proximity to the Earth. Experimental techniques for elucidating the scientific questions associated with the asteroids have been examined, and suitable experimental packages for the various missions outlined.

The guidance requirements for asteroid missions have been examined in some detail, as this is undoubtedly a critical area in the formulation of such missions. Specific calculations on the guidance requirements for the target bodies considered have been made, and the results are tabulated in an appendix. AUTHOR

Five missions in all have been considered, one to traverse the asteroid belt and measure solely the mass distribution, and the others to Eros, Ceres, Icarus, and Vesta. The importance of the preliminary 'fly-through' mission is stressed, so that spacecraft collision cross-sections may be calculated for subsequent missions. Three hypothetical launch vehicles are postulated, whose performance covers the range available with current generation vehicles. It is shown that landing missions using these vehicles to Eros, Ceres, and Vesta are possible, and the possibility of a return mission from Vesta is suggested.

A payload for any fly-by mission is compiled, taking into account power and transmission requirements, meteoroid shielding, guidance and control demands, spacecraft structure, and the experimental package. The necessity for terminal propulsion on Eros, Vesta, and Icarus missions is discussed, and the weight penalty involved is estimated. The addition of an extra high performance final stage for injection into the transfer conic orbit from a nominal 300 N. M. parking orbit is shown to increase the versatility of any launch vehicle significantly. A summary of the missions possible with and without this stage is given below.

POSSIBLE ASTEROID MISSIONS

Vehicle	Fly-By (lbs.)				Lander (lbs.)			
	Eros	Ceres	Icarus	Vesta	Eros	Ceres	Icarus	Vesta
Vehicle A (escape capability 500-750 lbs.)		--	600	--	--	--		--
Vehicle B (escape capability 2000-3000 lbs.)		--	2, 800	700	--	--		100
Vehicle C (escape capability 6000-7000 lbs.)	SEE TEXT	--	5, 500	1, 000	60	--	SEE TEXT	150
Vehicle A + High Performance Stage $I_{SP} = 440$		1, 000	3, 900	1, 300	400	130		200
Vehicle B + High Performance Stage $I_{SP} = 440$		1, 600	6, 600	2, 200	600	200		350
Vehicle C + High Performance Stage $I_{SP} = 440$		5, 500	23, 400	7, 300	2, 100	700		1, 100

TABLE OF CONTENTS

TABLE OF CONTENTS (Cont'd)

LIST OF FIGURES

LIST OF FIGURES (Cont'd)

APPENDIX

LIST OF TABLES

LIST OF TABLES (Cont'd)

A SURVEY OF MISSIONS TO THE ASTEROIDS

1. INTRODUCTION

The Asteroids, or Minor Planets, present a number of basic questions of major scientific interest, both as applied to the origin of the solar system, and to the evolution of the asteroid belt itself. In addition, investigation of the collision cross-section between the dust in the belt and future space vehicles is essential before missions to the outer planets can be considered. Not only is the distribution of small particles in the belt unknown, but the incidence of large bodies, of diameter 100-1000 meters is also the subject of much speculation.[1, 2] On the basis of the sparse data available it has been hypothesized that 10^5 to 10^6 bodies in the range 100-1000 meters diameter pass within 0.2 AU of the Earth every year[3], and this is over 2 AU from the center of the asteroid belt.

This report is the second in a series of studies intended to provide an outline of possible missions to targets within the solar system. It is aimed at providing sufficient depth to reveal the basic difficulties and critical areas associated with such missions, and to enable an overall comparative appraisal of the various mission configurations to be made. It is not intended however that this report be considered as a detailed mission study in which the consideration of trade-off parameters and optimization techniques has been pursued to its logical conclusion.

Preceding these reports on missions to specific targets is a second series of reports dealing exclusively with the scientific questions associated with the targets. This report will draw heavily from the results of its companion volume "The Scientific Objectives of Deep Space Exploration"[4]. However, the results of this latter document are summarized here for completeness, and in addition the orbital and physical data for some of the better known asteroids are listed in Tables 1 and 2.

Table 1

ORBITAL ELEMENTS FOR SOME ASTEROIDS (according to E. L. Krinov)

Cat. No.	Name	Year of Discovery	Diameter (miles)	Opposition Magnitude	Semi-Major Axis of Orbit (AU)	Orbital Period (years)	Eccentricity	Inclination of Orbit (deg)
1	Ceres	1801	478.5	7.4	2.767	4.6	0.0802	10.60
2	Pallas	1802	304.5	8.0	2.770	4.61	0.2394	34.82
3	Juno	1804	118	8.7	2.670	4.36	0.2574	13.02
4	Vesta	1807	236	6.5	2.361	3.63	0.0889	7.14
5	Astraea	1845	49.7	9.9	2.577	4.13	0.1862	5.33
6	Hebe	1847	69.6	7.0	2.42	3.77	0.2019	11.65
7	Iris	1847	77.7	6.7	2.386	3.69	0.2309	5.47
8	Flora	1847	56	7.8	2.201	3.27	0.1567	5.88
9	Metis	1848	77.7	8.1	2.387	3.69	0.1233	5.60
12	Victoria	1850	37.3	8.1	2.334	3.57	0.2190	8.38
15	Eunomia	1851	?	7.4	2.644	4.30	0.1870	11.76
18	Melpomene	1852	59	7.7	2.296	3.48	0.2176	10.15
20	Massalia	1852	65.9	8.2	2.409	3.74	0.1426	0.68
192	Nausicaa	1879	46.6	7.5	2.403	3.72	0.2445	6.87
324	Bamberga	1892	59	7.3	2.68	4.39	0.3346	11.30
387	Aquitania	1894	66.5	8.2	2.74	4.53	0.2383	17.97
433	Eros	1898	15.5	7.2	1.458	1.76	0.2230	10.83
719	Albert	1911	2.5	12.0	2.58	4.16	0.54	10.82
851	Wladilena	1920	?	12.7	2.362	3.63	0.274	23.0
944	Hidalgo	1920	21.7	11.0	5.71	13.7	0.65	43.06
1036	Ganymede	1924	?	12.5	2.665	4.35	0.54	26.2
1221	Amor	1932	1.6	16.0	1.973	2.77	0.45	----
----	Apollo	1932	1.2	17.0	1.486	1.81	0.566	6.4
----	Adonis	1936	0.6	19.0	1.969	2.76	0.78	1.5
----	Hermes	1937	0.9	18.0	1.290	1.47	0.474	4.7
1566	Icarus	1949	0.9	12.6*	1.078	1.12	0.827	23.0

* In closest proximity to Earth.

Table 2

PHYSICAL DATA OF SOME MINOR PLANETS COMPILED BY NIKOLAUS RICHTER FOR DIE STERNE, 36, 125 (1960)

No.	Cat. No. and Name	Light Variation: Max. amplitude	Light Variation: Period	Photographic Color Index	Phase Coefficient	Photographic Brightness for $r = 1$, $\Delta = 1$, $a = 4°$	Diameter (miles)	Albedo
1	(1) Ceres	$0\overset{m}{.}04$	9^h 05^m		0.045	$4\overset{m}{.}00$	477	0.032
2	(2) Pallas	0.13	5^h-6^h or 10^h-12^h	$0\overset{m}{.}50$	0.036	4.99	306	0.052
3	(3) Juno	0.15	7^h $12\overset{m}{.}6$	0.83	0.036	6.36	127	0.115
				0.55				
4	(4) Vesta	0.13	5 20.5	0.67	0.026	4.20	244	0.252
			10 41.0	0.70				
				0.68				
5	(6) Hebe	0.16	7 17	1.20	0.032	6.60		
6	(7) Iris	0.29	7 08.1	0.55	0.019	6.76		
			7 03					
7	(8) Flora	0.04	≈13 36	0.97	0.028	7.45		
8	(9) Metis	0.26	5 04.6	0.95	0.044	7.17		
9	(10) Hygeia	0.10	18 ?	0.84	0.066	6.45		
10	(11) Parthenope	0.07	≈10 40	1.54	0.030	7.67		
				0.86				
11	(14) Irene	0.035	11 ?	1.30	0.034	7.31		
12	(15) Eunomia	0.53	6 05.0		0.042	6.08		
13	(16) Psyche	0.12	4 18.2	1.11	0.030	6.74		
14	(17) Thetis	0.36	12 16.5	0.50	0.040	8.59		
15	(20) Massalia	0.20	8 05.9	0.48		7.38		
				0.66				
16	(22) Calliope	0.14	4 09			7.35		
17	(25) Phocaea	0.18	9 56.7		0.025	8.98		

Table 2 (Cont'd)

No.	Cat. No. and Name	Max. amplitude	Period	Photographic Color Index	Phase Coefficient	Photographic Brightness for r = 1, Δ = 1, α = 4°	Diameter (miles)	Albedo
18	(39) Laetitia	0.53	5 08.3 11 09.5	0.82 0.36	0.022	7.30		
19	(44) Nysa	0.43	6 25.2	0.75	0.028	7.91		
20	(321) Florentina	0.40	2 52.2		0.030	11.26		
21	(354) Eleonora	0.15	4 16	0.77		7.47		
22	(433) Eros	1.5	2 38		0.024	12.31		
23	(511) Davida	0.25	5 13, 5^h07^m			7.02		
24	(532) Herculina	0.08	16^h-17^h	0.94		7.88		

2. THE SCIENTIFIC QUESTIONS ASSOCIATED WITH THE ASTEROIDS

The origin and nature of the asteroids has been the subject of much speculation, leading to a variety of scientific questions, which, when answered will lead to a more informed opinion on the origin of the solar system. The most important of these questions (from a purely scientific point of view) are as follows:

a. Are any of the larger minor planets original planetary condensations?

b. What is the chemical constitution of the asteroid belt?

c. What is the mass distribution of the belt?

d. Is there a distinct connection between the asteroids and the meteorites?

e. What is the density of the asteroids, especially the larger bodies?

f. Can evidence of the degree of accretion of particles in the belt be found? In particular can any of the larger bodies be shown to have origin by accretion?

g. What is the age of the asteroid belt?

h. Is there any evidence for a biological history on the asteroids?

i. Is there a magnetic field associated with the asteroids?

j. What is the nature of the surface of the asteroids?

According to Kuiper, any body of asteroidal mass with small eccentricity and inclination whose orbit lies within 4 AU, must have been within that limit ever since the mass of Jupiter reached its present value.

One added reason for investigating bodies like Ceres, Pallas, or Vesta therefore, which have orbits inside 4 AU, is that doing so increases the probability of the asteroid under examination being an original member of the belt.

The asteroids suspected of being collision fragments, in general, are harder to detect because of their smaller size, with the one notable exception of Juno (204 km) which orbits between 2 and 3. 3 AU. It should be noted that evidence of fragmentation among asteroid bodies is given by the variation in the apparent magnitude of the body as it rotates. This variation, it could be argued, would occur if the asteroid had a patchy surface with widely differing albedos. Such an interpretation would necessitate an accompanying change in color with rotation, which however, has not been observed[5], and therefore, the interpretation that these bodies must be irregularly shaped is widely accepted.

The bulk of the asteroid mass known so far lies between 2 and 3. 5 AU, with orbital inclinations mostly between + 10° as demonstrated in Figures 1 and 2. Approximately one third of this mass is known to be taken up by the largest body, Ceres.

It is generally agreed that whatever mechanism is chosen for the origin of the asteroids, there has since been a continuous grinding process by multiple collisions, in particular Piotrowsky[6] has calculated the collision probability for asteroids of varying size, inclination and eccentricity. This process, he concludes, leads to the regeneration of the smaller particle population, which would otherwise have been cleared by the Poynting-Robertson effect, by which small particles are gradually caused to spiral into the Sun.

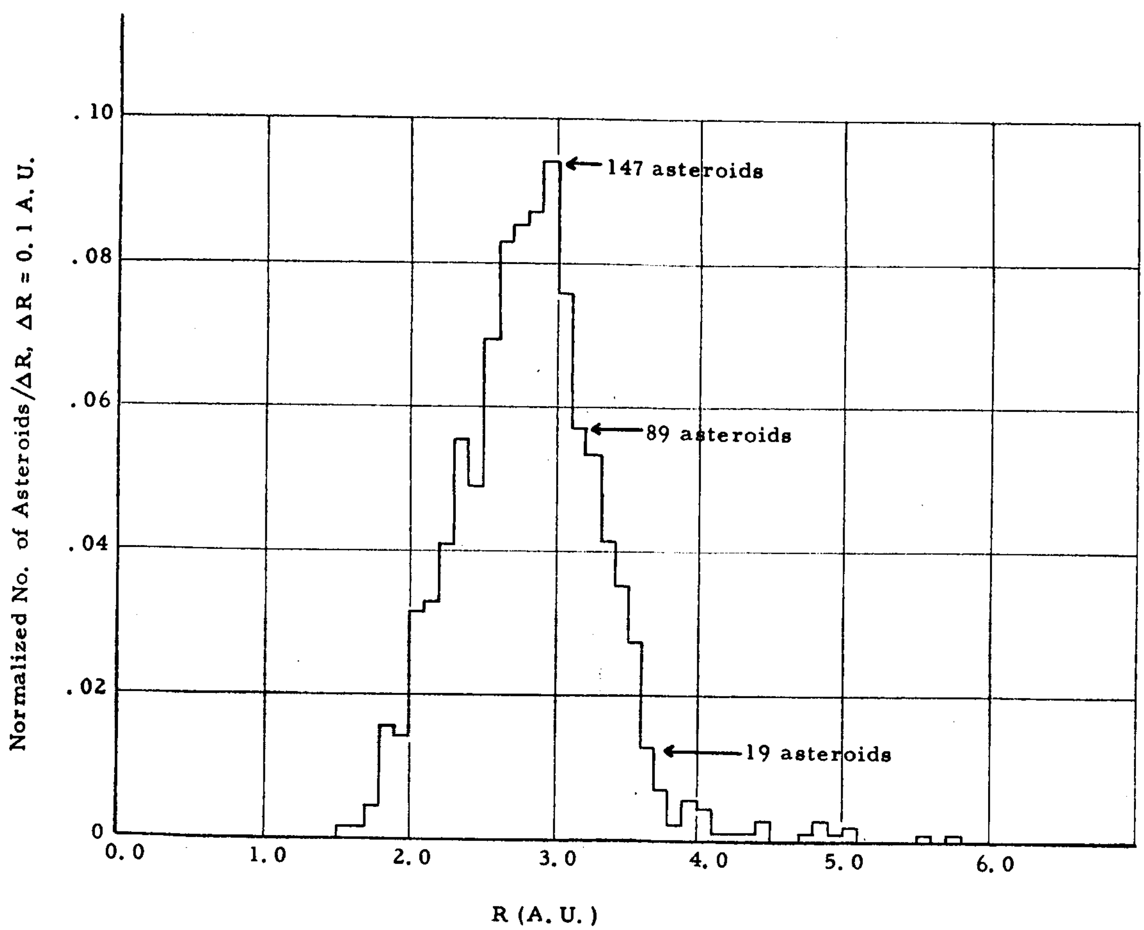

Fig. 1 1563 NUMBERED ASTEROIDS GROUPED TOGETHER BY DISTANCE FROM THE SUN: No. OF ASTEROIDS PER GROUP VS DISTANCE FROM THE SUN ON 1/1/65

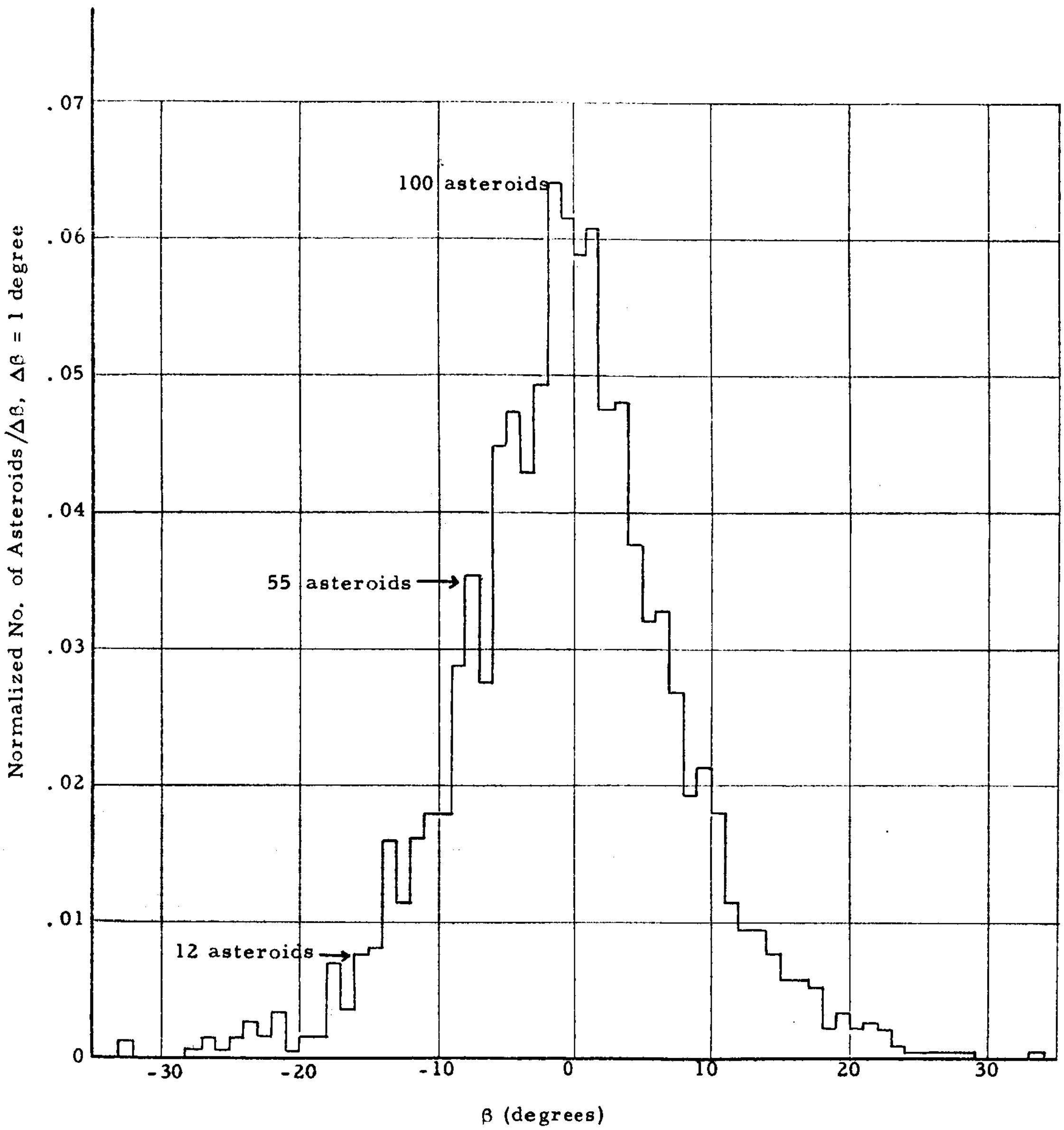

Fig. 2 1563 NUMBERED ASTEROIDS GROUPED TOGETHER BY HELIOCENTRIC LATITUDE: No. OF ASTEROIDS PER GROUP VS LATITUDE OF THE GROUP ON 1/1/65

Considerable evidence is accumulating to indicate the presence of large collision fragments in the belt, and the verification of their presence by a space probe, although a major achievement would not by itself cause a great deal of surprise in the scientific world. What would be of interest however, on such a mission, would be the study of the fragmented surface, and the effects of cosmic and asteroidal erosion. It seems doubtful whether an examination by a fly-by experiment of such a surface could reveal information about anything more than the first few centimeters of surface depth.

The age of the asteroid belt since fragmentation is a parameter not open to direct scientific measurement, although measurement by interference is certainly a possibility, using the degree of surface erosion, or the radioactivity of the bodies as a guide.

In view of the many experiments[7] to establish the presence of biological organisms in the chondritic meteorites, and the long association between meteorites and the asteroid belt it would be of extreme interest to detect the presence of a biological history on the asteroids. This investigation could only be performed by a fairly sophisticated analysis of asteroidal material, which is best conducted by a lander, since the sample collected by any other type of mission would be small and of mixed origin.

It would be of considerable interest to be able to measure the mass and size, and hence the density, of any of the asteroids. From this information, an informed guess could be made as to the composition and structure of the bodies, and consequently their origin.

The major objectives of any mission family to the asteroid belt can be listed as follows:

a. To determine the mass distribution in the belt.

b. To detect an original non-fragmented major asteroidal body, and obtain information about its internal construction and mass.

c. To inspect an asteroid suspected of being a collision fragment, either by fly-by or lander, determine its surface erosion since fragmentation, density and internal construction and mass.

d. To analyze a sample of asteroidal matter, determine its chemical constituion (and density).

e. To find evidence for the existence of a biological history in the belt, (detection of hydrocarbons, organic acids, etc.)

2.1 Possible Experiments for Asteroid Missions

The following experiments are suggested as being necessary to accomplish the scientific objectives outlined in the previous section.

a. Experiments to determine mass distribution

b. Optical experiments

c. Radar experiments

d. Chemical analysis of the dust particles, for both organic and inorganic constituents

e. Television

f. Seismic experiments

g. Mass and density measurement

h. Magnetic measurements

i. Temperature measurements

2.1.1 Measurement of Mass Distribution

It has been suggested[8] that the collision cross-section for a spacecraft passing through the belt could be determined by tracking optically the passage of one or more passive balloon type probes injected into the belt, and noting the perturbations produced by collision with asteroidal particles in its trajectory. This concept is discussed in Appendix I, where it is concluded that an entirely passive system would not be an economical configuration.

A more efficient method of utilizing a given payload would be to employ a balloon of the type that hardens under exposure to the space environment and use its surface as a diaphragm for a conventional micrometeorite counter, telemetering the information back. This configuration merely uses the balloon to increase the encounter probability.

The dynamic range of micrometeorite energy measuring instruments is decidedly limited. The actual number of particles encountered is of course a function of the particle size. Assuming the majority of the asteroidal mass not accounted for by Ceres is invested in dust particles, the variation of encounter rate with particle size is as follows (see page 35).

Particle size	Encounter rate per square meter of spacecraft frontal area *
10 μ	4,000/sec
100 μ	4/sec
1 mm	10/hr
1 cm	20/week

* Density assumed to be that of the stony meteorites.

It can be seen that the collision probability is a steep function of the particle size, and a practical figure can only be derived by assuming that which one is trying to investigate, namely the particle size distribution, or alternatively using a particle detector of very wide dynamic range.

Conventional micrometeorite detection can of course be employed, but unless a large collector area is used (say 2 square meters), the risk remains of encountering too small a number of particles to give a clear indication of the mass distribution. This would certainly happen if the distribution is weighted away from the smaller particle sizes.

2.1.2 Optical Experiments

Measurement of the size and population of small particles by photometric and polarization experiments has been well illustrated by the many observations conducted on the zodiacal light,[9] in which the sunlight scattered from dust particles inside the earth's orbit, 3μ to 300μ in size is examined for spectral anomalies, and polarization. The density of these particles is of the order 10^{-14} particles $/cm^3$. To postulate the same order of particle densities in the asteroid belt, one only has to assume that 10^{-4} to 10^{-3} of the total asteroidal mass is invested in small particles (with distribution centered around 100μ say), an assumption which does not seem unreasonable. The inclusion of a spectrometer and photometer in the experimental package to measure the difference between the forward scattered light and the incident sunlight, can be used to provide information on the density of very small particles (of the order of the wavelength of the incident light, 0.1 to 0.5μ). Although the solar intensity at 3 AU is only one ninth of that on Earth, the intensity of forward scattered light should still be sufficient for measurements, especially since the particle density will if anything increase as the asteroid belt is approached.

Once inside the belt, detection of larger bodies becomes a problem which is probably best solved by either radar, or its optical equivalent using a pulsed laser transmitter. The inclusion of a radar type of experiment can serve other uses as well.

2.1.3 Radar Experiments

The inclusion of an experiment using radar principles is not difficult to justify on any asteroid mission. Firstly, range data at target encounter coupled with the angular diameter presented to the spacecraft, is essential in order to calculate the physical size of the body. The same instrument is capable of providing altitude and rate of descent data for a lander mission, which enables the mass and density of the body to be calculated, thus obtaining considerable scientific knowledge with the one instrument.

There appears to be no reason why the same experiment commanded into a cruise mode should not examine the distribution of large particles. By slightly defocussing the antenna feed, (or interposing a convex lens in the case of a laser), the field of view can be made as broad as is desired at the expense of useful range, without the inclusion of a separate steering mechanism for the antenna, since in the encounter mode, the whole spacecraft would almost certainly be required to 'look' at the asteroid, to enable spectrographic and radiometric measurements to be made.

However, scanning radars are well within the state of the art, and the only reason for excluding a scan capability on such a radar would be to conserve payload space weight or power. The usefulness of this technique is examined in Appendix II, and the results of the calculation appear in Table 3.

2.1.4 Chemical Constitution

Analysis of the dust and small particles in the asteroid belt, or better still, analysis of material from a larger solid body is an objective of prime scientific interest, providing considerable evidence for the long association of meteorites with asteroids, and even more important, giving significant data from which the theories concerning the history and origin of the asteroids may be substantiated.

A variety of techniques are available for this analysis, some of the most suitable are listed below:

(a) Thermal neutron activation, in which the sample is irradiated from a neutron source, and the gamma ray spectrum due to the artificially induced radioactivity is subsequently analyzed, thus enabling the atomic constituents in the sample to be identified.

(b) Neutron capture gamma ray analysis, in which the sample is irradiated by an intense source of neutrons (10^4 - 10^8 /cm^2. sec) and the capture gamma ray spectrum observed simultaneously. This method identifies most of the atomic constituents present in meteorites with ease[(10)], in particular, the presence of hydrogen (and therefore water) is detectable with concentrations of 1 part in 10^4 by weight.

(c) Differential thermal analysis, in which the sample is heated and allowed to cool, its temperature being carefully measured throughout the cycle. In this experiment compounds are identified by the effects of their phase changes on the temperature gradient.

Table 3

THE SENSITIVITY OF A 1 KW PULSED RADAR SYSTEM WITH 35 DB ANTENNA

Radius of Viewing Circle	Range	Particle size	Name if any
190 meters	3.8 km	1 cm	
600 meters	12 km	10 cm	
1.9 km	38 km	1 meter	
75 km	1500 km	1.4 km	Icarus
350 km	7000 km	22 km	Eros
1,500 km	30,000 km	380 km	Vesta
2,250 km	45,000 km	765 km	Ceres

(d) Gas chromatography, in which the sample has to be transferred to a sealed system and heated to several hundred degrees Centigrade. Any volatile components in the sample vaporize, the vapor being forced through a series of analytical columns, where their passage is impeded for an interval of time unique to each component. This technique is particularly sensitive to the presence of organic compounds, the minimum detectable quantity being 3×10^{-10} gm molecules for some 30 organic compounds, and the dynamic range of the instrument being 10^4. An experiment of this type has already been developed for the Surveyor project.[11]

(e) X-ray fluorescence, in which the sample is bombarded with x-rays of suitably high energy to excite electron transitions in the sample (notably K and L shell transitions). The emission (fluorescent) spectrum generated as the electrons return to their unexcited state identifies the elements present. The method is capable of detecting elements occurring in the sample to the extent of 1 part in 10^6.

(f) Alpha Scattering, in which the sample is bombarded with alpha particles, and the energy spectrum of the scattered particles is measured. From this spectrum, an analysis of the elements present in the sample is possible. The technique suffers from extreme sensitivity to sample contamination however. In addition the presence of any residual atmosphere (greater than 10μ Hg) would also produce errors in the experimental results. Finally the method only analyzes the top few microns of the sample, and therefore sample manipulation is again called for.

Other methods are possible but suffer from characteristics which make them unsuitable for an asteroid mission. Among these are x-ray diffraction which is particularly suited to analysis of crystalline materials; and mass spectrometry and emission spectroscopy both of which would require considerable manipulation of the sample.

Of the techniques considered, neutron capture gamma ray analysis appears to be promising for inorganic analysis, being both sensitive and reliable. For the detection of organic compounds, the gas chromatography experiment has by far the most impressive capability.

One important parameter however which will affect the choice of experiment is the degree of sample manipulation entailed in each technique, and in this respect gas chromatography does not show up in a good light.

2.1.5 Television

The details of a television subsystem for an asteroid mission depend solely on how close the spacecraft can approach the target, and the amount of observation time available after encounter. It has been suggested that the observation time should be extended as much as possible by the use of terminal maneuvers, but in the case of Ceres for example, the approach velocity is so high that to reduce it to zero would very possibly be uneconomical, and so in this case would require a high speed, high sensitivity television system (probably image orthocon) to make the usable observation time a maximum. The resolution required is very much a function of the target under consideration. While a 1 km element may be highly informative for Ceres, the same resolution would not be sufficient for Eros, where it is details of the fragmental surface that are of interest and the target body is small anyway.

If one assumes a miss distance of 1,000 km for an Eros fly-by for example, a modest system, using a 512 line orthocon tube, and working at a focal length of 44 cm, would have a resolution of 100 meters at the surface of the asteroid. By using more sophisticated optics this could be reduced to 10 meters without undue difficulty. The development of promising new image tubes (e. g., the secondary electron conduction vidicon) with very low illumination requirements means that these higher resolution systems involving long focal lengths can be achieved without resorting to physically large apertures and therefore heavy camera systems.

For a body the size of Ceres ($\sim$760 km) the gross surface features; maria, craters, rifts etc., could be identified from a much greater distance with the above system. To attain similar resolution to that presently attainable on the lunar surface, ($\sim$1 km) a miss distance less than 100,000 km sufficient, in conjunction with a 440 cm optical system is required. With the advent of Ranger, Surveyor, and Voyager, such flyable systems appear to be well within the state of the art.

2.1.6 Seismic Experiments

Seismic experiments, from an asteroid lander are, in theory, capable of indicating the presence of an asteroidal crust, or core, or both, and of measuring the density distribution with depth. Microseismic activity should provide some measure of the thermal stresses generated as the body rotates in sunlight. Meteoric impacts may also provide sufficient excitation to enable their frequency to be detected. Since there is no detectable atmosphere on the asteroids, and hence no weather, the microseismic noise level will be low, making possible the use of high magnification instruments. The actual performance figures, frequency passband, sensitivity will depend very much on the size of the target asteroid, and the method of landing and deploying the seismometer. A seismometer suitable for hard landing on the surface of the Moon as discussed in detail by Lehner et al[12], and it is concluded that an instrument having a gain greater than 10^6 can be constructed to withstand landing shocks of 3000 G, and yet weigh less than 5 lbs.

2.1.7 Mass and Density Measurement

Since the spacecraft will be in free fall conditions on encounter, conventional gravimeters will not be feasible. The mass of a given asteroid can be deduced however from the acceleration of the spacecraft towards it after the terminal maneuver. This, in turn, can be calculated from the radar altimeter readings. Simultaneous optical measurements on the asteroid's size yields sufficient data to calculate the density.

2.1.8 Magnetometers

Measurement of the interplanetary magnetic field is always of considerable interest, since no really substantial measurements with a supporting theory are available as yet. The magnetometer would therefore serve the dual purpose of detecting any turbulence in the magnetic field between 1 AU and 3.5 AU and would also detect any trapped magnetic field in the target asteroid. The instrument suggested in the Rubidium Vapor Magnetometer, which handles a range of $1\,\gamma$ to $300\,\gamma$ without undue difficulty.

2.1.9 Temperature Measurement

The equilibrium temperatures of rotating bodies with no internal heating in the asteroid belt range typically from 140° K to 200° K, and may be conveniently measured by a microwave radiometer working in the region 1 mm to 20 mm.

Table 4

SUMMARY OF POSSIBLE EXPERIMENTS FOR ASTEROID MISSIONS

Experiment	Mass	Average Power Consumption
1. Photometer to detect small particles	10 lbs.	5 W (1000-5000 Å)
2. X-Band radar altimeter and large particle detector + 35 db antenna	30 lbs.	15 W (X-Band) continuous
3. Neutron capture gamma ray analyzer	40 lbs.	10 W
4. Gas chromatograph	15 lbs.	15 W
5. Television (512 lines, 440 cm, focal length optics)	25 lbs.	20 W
6. Seismic experiment	5 lbs.	5 W
7. Magnetometer	10 lbs.	5 W
8. Microwave radiometer	10 lbs.	1 W
Total	145 lbs.	76 W

3. GUIDANCE FOR ASTEROID MISSIONS

3.1 General Considerations

As interplanetary mission objectives become more demanding, the role played by guidance becomes increasingly complex and significant. The asteroid mission presents a case in point. Basically, the function of guidance is to insure delivery of the mission payload to the near vicinity of the target asteroid within an accuracy tolerance consistent with meeting the specified scientific objectives. Such objectives would normally require that the payload be placed within several hundred to several thousand kilometers from the surface of the asteroid, and that its relative motion at this position be essentially zero. We are thus dealing with a sequence of guidance activities that may generally be termed intercept and rendezvous.

The accepted procedure of dividing the guidance problem into the injection, mid-course, and terminal phases is certainly valid in this case. The purpose of injection guidance is to establish the spacecraft on a coasting trajectory that will intercept the target asteroid in its orbit at a given time. Since the injection guidance system cannot be expected to perform perfectly, the errors incurred at injection will cause a subsequent deviation from the desired trajectory, thereby resulting in target position errors. It is not unreasonable to assume that, at least for some time to come, injection guidance will not be sufficiently accurate to permit the position errors to go uncorrected. Hence, it will be necessary to provide for one or several mid-course corrections in order to place the spacecraft back on course. It is expected that mid-course guidance can be accomplished, for the most part, by DSIF earth-based tracking, orbit determination, and command.

Although there does not appear to be a strong requirement for a completely self-contained mid-course guidance system, this point will require further examination.

In addition to providing for velocity matching at the target, terminal guidance may be required to correct the residual position errors remaining after the mid-course maneuver. These errors arise from three sources; tracking inaccuracy, inaccuracy in controlling the magnitude and direction of the mid-course impulse, and inaccurate knowledge of the asteroid's orbital parameters. This latter source of error will require special attention and considerable improvement. An intensified observational and orbital prediction effort will probably be required prior to an actual launch.

Terminal guidance takes place near the destination, say within one million kilometers, and is generally based on navigational observations of the asteroid. Here, the requirement for an on-board guidance system is in evidence. Perhaps the most difficult guidance problem associated with the asteroid mission will be related to the instrumentation required for detection and navigational measurements.

Guidance analysis has been undertaken within the scope of advanced mission studies in order to determine preliminary estimates of propulsion and sensor requirements, and to identify specific problem areas that should be studied in greater detail. A discussion of the mid-course and terminal guidance calculation is given in Appendix III, however a summary of the calculation as applied to four specific target bodies is presented in the following section.

3.2 Summary of Mid-Course Guidance Results for Missions to Ceres, Vesta, Icarus, and Eros

3.2.1 Injection Errors Assumed for Study

The proper way of determining injection (launch) errors is to conduct a detailed error analysis of the injection guidance system. This involves designating each source of hardware error and generating launch trajectories for each mission. Obviously, this type of complete simulation is not within the scope of the present study. The simpler method adopted was to assume errors in the hyperbolic excess velocity components. Two alternatives suggested themselves. The first was to assume error magnitudes proportional to the magnitude of the hyperbolic velocity for a given mission. The second was to assume constant error magnitudes for all missions. Obviously, neither alternative is truly representative of the actual case. It was decided that there was no strong justification for assuming the first alternative to be more representative, and therefore the conclusions drawn from the guidance study could possibly be misleading. On the other hand, designation of errors as in the second method yields results which are akin to basic error sensitivities, and since the analysis is linear, the results can be easily modified or adjusted. For example, if it were decided that the assumed injection errors are too small by a factor of 2, all the guidance results would then be multiplied by this factor. For this reason, the second alternative was chosen.

The injection errors assumed are

$$\Delta VHL_x = \Delta VHL_y = \Delta VHL_z = 10 \text{ m/sec RMS}$$

Each component statistically uncorrelated. Based on these assumptions, the uncorrected miss distances characteristic for missions to Ceres, Vesta, Icarus and Eros are shown in Figures through , and mid-course guidance requirements tabulated in Tables 5 through 8.

3.2.2 Significant Conclusions

a. For a given target asteroid and launch date, the uncorrected miss distance and the time-of-flight error generally increases with the time-of-flight. This result is as expected inasmuch as the longer flights correspond to transfer trajectories which are more sensitive to initial velocity errors.

b. Since constant injection errors are assumed for all missions, the mid-course ΔV required does not vary significantly from one mission to another. For all missions studied, the FTA correction lies within the range 16-23 m/sec, and the VTA correction within the range 13-20 m/sec.

c. The miss distance remaining after the mid-course correction is a function of three error sources: (1) DSIF tracking inaccuracy, (2) inaccurate knowledge of the asteroid orbital parameters, and (3) inaccuracy in applying the mid-course impulse. Data is not readily available concerning the effect of tracking inaccuracy as applied to asteroid missions. However, if the data available for the Mariner shot is representative, then the miss distance uncertainty (as a result of 10 days tracking and data smoothing) should be within 1000 km. The second error source has not been studied. The third error source has not been studied in detail, however approximate results can be obtained from the figures. As an example, consider the 200 day

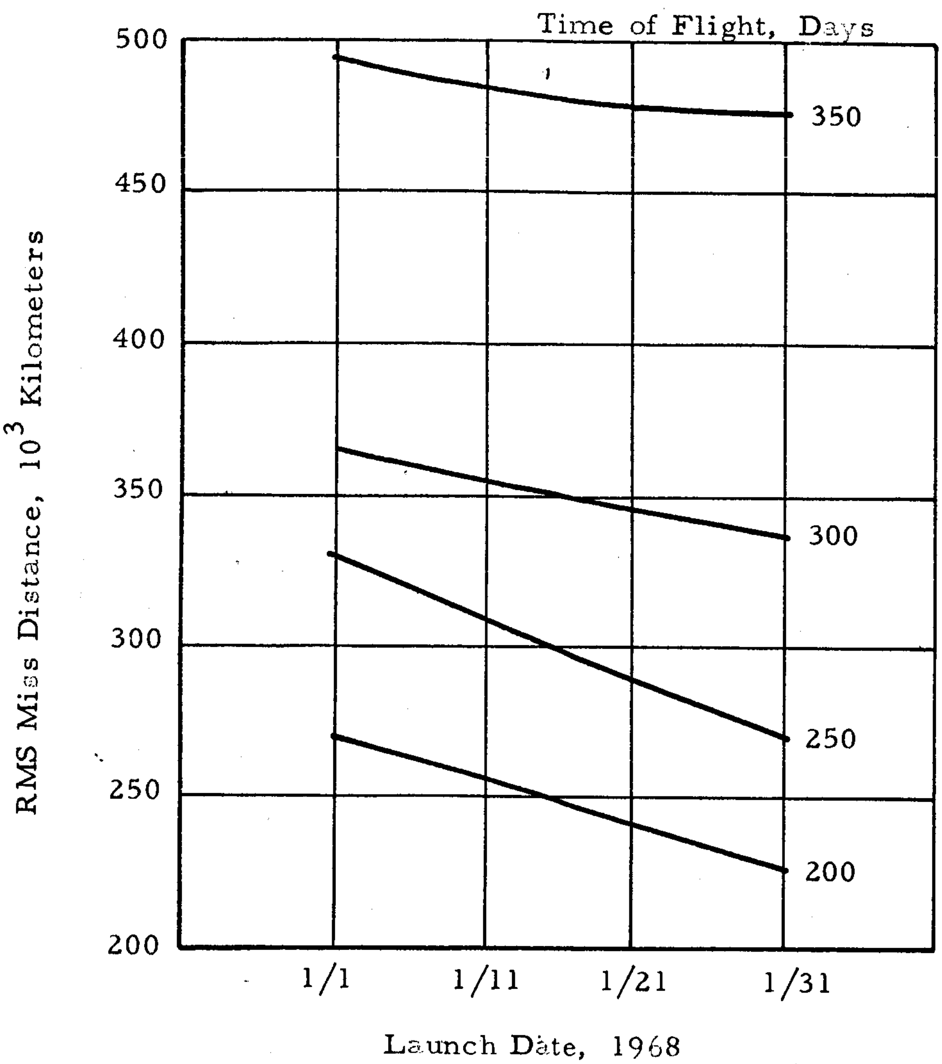

Fig. 3 UNCORRECTED MISS DISTANCE CHARACTERISTIC FOR CERES MISSIONS

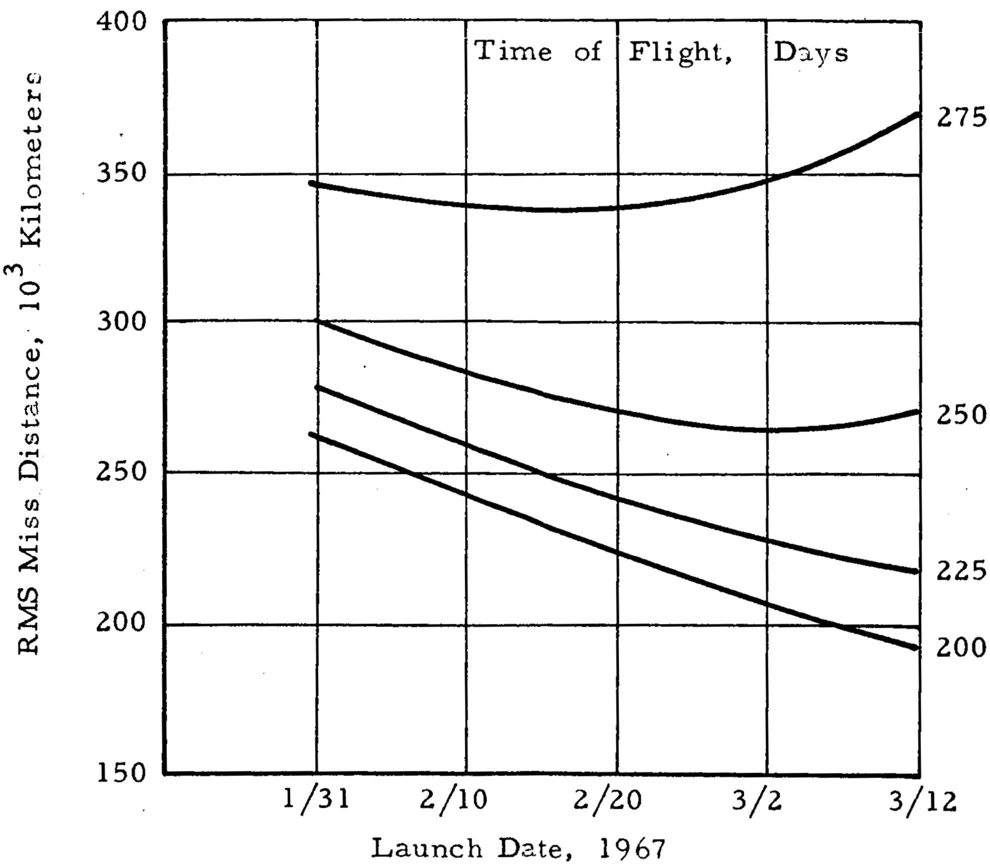

Fig. 4 UNCORRECTED MISS DISTANCE CHARACTERISTIC FOR VESTA MISSIONS

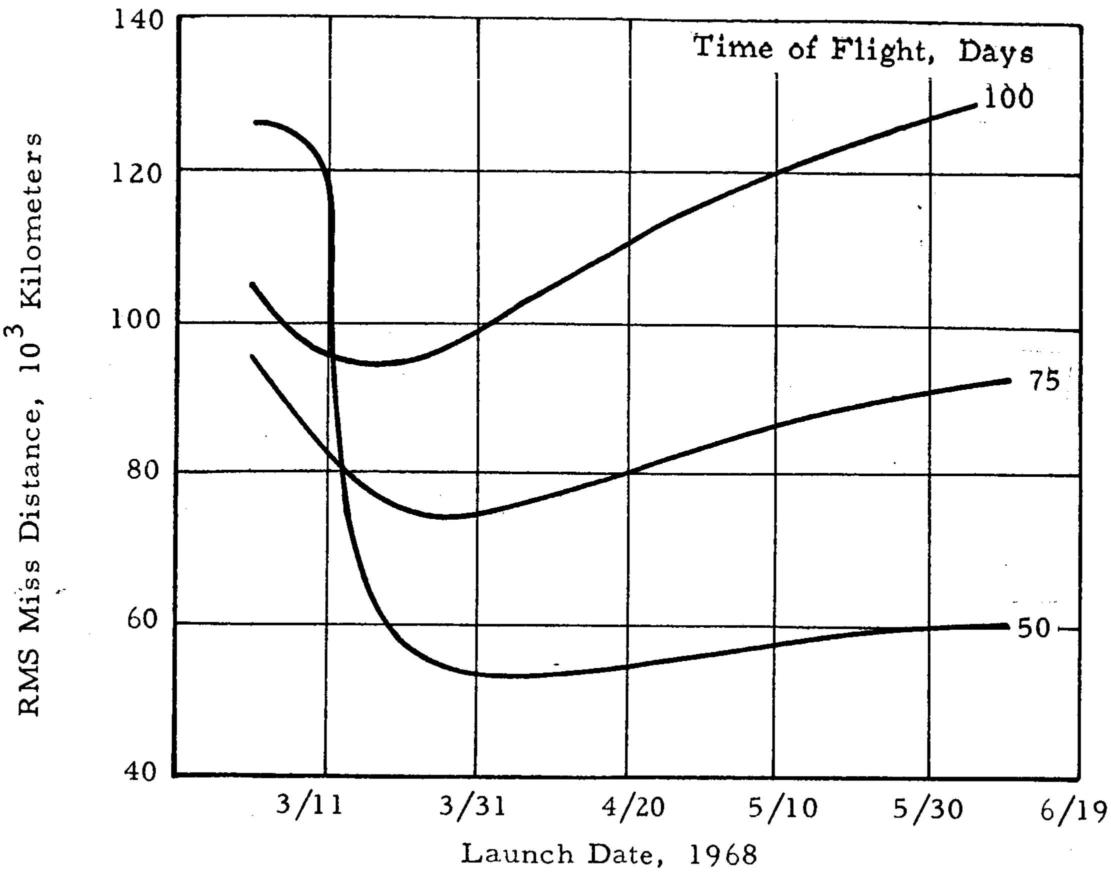

Fig. 5 UNCORRECTED MISS DISTANCE CHARACTERISTIC FOR ICARUS MISSIONS

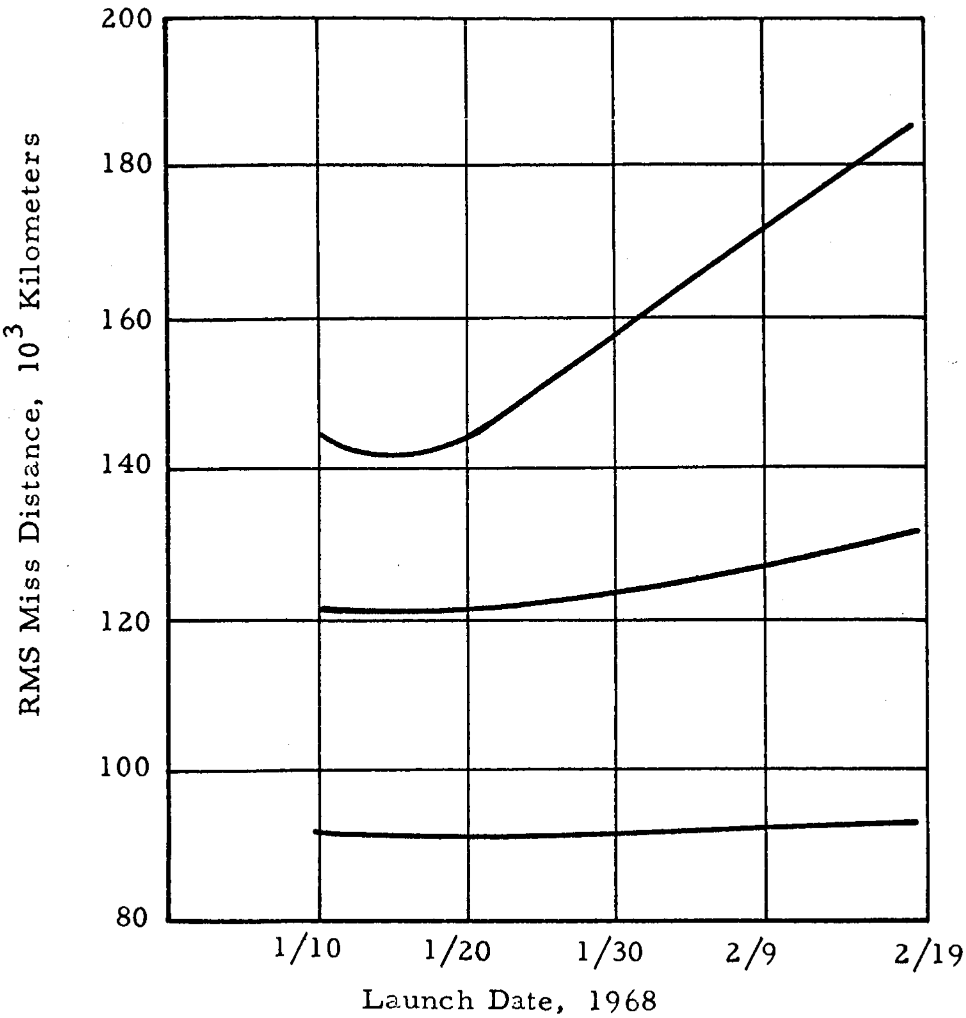

Fig. 6 UNCORRECTED MISS DISTANCE CHARACTERISTIC FOR EROS MISSIONS

Table 5

MIDCOURSE GUIDANCE FOR CERES MISSIONS

Time of Flight Days	Launch Date	Uncorrected Target Errors			Midcourse Velocity Correction, m/sec	
		Δb, 10^3 km	Δ TF, min	ΔVHP, m/sec	ΔV_c - FTA	ΔV_c - VTA
200	1/1/68	270	289	28.2	17.6	13.3
	1/11	255	303	27.7	17.8	13.5
	1/21	240	320	27.2	17.9	13.8
	1/31	226	339	26.7	18.0	14.0
300	1/1	365	1280	43.5	16.7	14.0
	1/11	357	1290	41.8	16.9	14.4
	1/21	346	1300	40.0	17.1	14.7
	1/31	337	1320	38.1	17.3	14.9
350	1/1	494	1970	43.5	16.1	14.8
	1/11	485	1970	41.8	16.5	14.8
	1/21	478	1970	39.9	16.8	14.8
	1/31	478	1960	37.5	16.9	14.7

* All results are RMS

** Midcourse correction made at 10 days from launch

Table 6

MIDCOURSE GUIDANCE FOR VESTA MISSIONS

Time of Flight Days	Launch Date	Uncorrected Target Errors			Midcourse Velocity Correction, m/sec	
		Δb, 10^3 km	ΔTF, min	ΔVHP, m/sec	ΔV_c - FTA	ΔV_c - VTA
200	1/31/67	261	504	38.2	17.5	13.3
	2/10	243	540	37.4	17.6	13.7
	2/20	224	579	36.6	17.7	14.1
	3/2	207	621	35.5	17.8	14.6
	3/12	193	662	34.2	17.9	15.0
250	1/31	299	1200	46.4	16.8	14.7
	2/10	285	1240	44.5	17.0	14.8
	2/20	270	1280	42.4	17.2	15.1
	3/2	264	1310	39.8	17.3	15.0
	3/12	271	1320	36.6	17.4	14.7
275	1/31	345	1580	45.5	16.4	14.9
	2/10	338	1610	43.3	16.7	14.8
	2/20	338	1630	40.5	16.9	14.7
	3/2	348	1630	37.2	17.1	14.5
	3/12	371	1580	33.2	17.2	14.1

* All results are RMS

** Midcourse correction made at 10 days from launch

Table 7

MIDCOURSE GUIDANCE FOR ICARUS MISSIONS

		Uncorrected Target Errors			Midcourse Velocity Correction, m/sec	
Time of Flight Days	Launch Date	Δb, 10^3 km	ΔTF, min	ΔVHP, m/sec	ΔV_c - FTA	ΔV_c - VTA
50	3/1/68	126	8.61	63.2	23.2	19.5
	3/21	57.1	11.2	64.2	21.5	16.9
	4/10	53.3	20.9	22.5	21.6	17.5
	4/30	55.9	32.8	15.6	21.6	17.7
	5/20	58.6	55.9	12.6	21.6	17.7
	6/9	60.8	211	10.7	21.7	17.8
75	3/1	95.5	27.0	81.8	19.7	15.2
	3/21	75.7	45.3	33.3	19.8	15.7
	4/10	76.6	64.2	22.1	19.9	16.3
	4/30	83.5	85.7	16.3	19.9	16.4
	5/20	88.7	134	13.0	20.0	16.4
	6/9	93.1	477	10.6	20.0	16.5
100	3/1	105	81.7	45.0	18.9	14.5
	3/21	94.3	110	30.0	19.0	15.3
	4/10	105	133	21.4	19.1	15.8
	4/30	116	162	16.0	19.2	15.9
	5/20	123	241	12.8	19.2	15.8
	6/9	130	822	10.0	19.2	15.9

* All results are RMS
** Midcourse correction made at 10 days from launch

Table 8

MIDCOURSE GUIDANCE FOR EROS MISSIONS

Time of Flight Days	Launch Date	Uncorrected Target Errors			Midcourse Velocity Correction, m/sec	
		Δb, 10^3 km	Δ TF, min	ΔVHP, m/sec	ΔV_c - FTA	ΔV_c - VTA
75	1/10/68	91.4	205	19.1	19.9	16.3
	1/20	90.8	219	18.4	19.9	16.4
	1/30	91.1	226	17.2	20.0	16.5
	2/9	91.7	225	15.9	20.0	16.6
	2/19	92.7	216	14.4	20.0	16.7
100	1/10	121	498	27.1	19.1	15.4
	1/20	121	535	25.5	19.1	15.5
	1/30	123	536	23.0	19.1	15.8
	2/9	127	500	19.8	19.1	16.0
	2/19	132	443	16.5	19.2	16.1
125	1/10	145	1080	35.5	18.5	14.8
	1/20	144	1210	33.5	18.6	14.9
	1/30	157	1150	28.7	18.6	15.4
	2/9	173	947	22.4	18.6	15.7
	2/19	185	730	16.5	18.7	15.8

* All results are RMS

** Midcourse correction made at 10 days from launch

Ceres mission having a launch date of 1/11/68. From Figure 3, the miss distance sensitivity to a mid-course ΔV error is of the order

$$\frac{255,000}{17.8} \frac{km}{m/sec} = 14,300 \frac{km}{m/sec}$$

Now, assuming a ΔV error of 0.1 per cent, the miss distance remaining after the correction would be 255 km. Although this analysis is somewhat crude, order-of-magnitude results can be obtained.

4. MISSIONS TO THE ASTEROIDS

4.1 General Considerations

On examining a variety of missions to the asteroids it is soon discovered that there is a wide range of values for launch energy, approach velocity at encounter, target body size, and in fact all the parameters associated with a mission study. It is true therefore to say that one cannot outline a generalized mission to the asteroids, since even the configuration of the mission, fly-by, lander, or orbiter, which provides the most efficient information return in terms of payload weight, may vary from asteroid to asteroid. There are however some features which are common to many missions.

On examining optimum trajectories to the asteroids one common feature that becomes apparent is the consistently high values of VHP, the asymptotic approach velocity at encounter. For the larger asteroids, this limits the observation time severely, and for the smaller bodies, makes observation practically impossible. It also has the effect of making target acquisition more difficult. Vesta for example, one of the less difficult bodies to acquire on account of its size, moves at 2° /min for a miss distance of 40,000 km and a VHP of 10 km/sec. (If, like Mariner 2, the spacecraft passes within 5.5 target radii, then the figure for Vesta increases to 34° /min.)

The point to be made here is that unless the spacecraft experiments, attitude control, and target sensors are capable of rapid response and high scan rates, some method of reducing the angular passage of the target at encounter must be found. Reduction of VHP by a terminal maneuver seems an obvious choice, although this does impose severe weight penalties on the payload. It should be noted that the smaller the body, the more VHP has to be reduced in order to extend the viewing time, and the more favorable conditions become for a lander type of spacecraft.

A further consideration to be applied to all missions actually penetrating the asteroid belt, is that there is liable to be a high meteoroid impact rate. The possibility of a high erosion rate indicates that solar cell power supplies would not be a good choice, a better alternative being an isotopic power supply. For missions to asteroids involving near Earth encounter (Eros, Icarus), this argument does not apply.

The question of how much meteorite shielding is needed for asteroid missions has been discussed in the literature[13, 14], and it only remains to point out that by careful design, the structural elements themselves can be used to partially protect the vulnerable parts of the spacecraft, and so reduce extra shielding to a minimum.

The following section outlines five possible missions, two of which intercept the target bodies close to Earth, two in the main belt, and one mission to determine the mass distribution in the belt without any particular target body. This last, a "fly-through" mission, is particularly attractive as a first mission, since it provides data essential to the design of future spacecraft to targets beyond 2 AU, needs no guidance, and has no launch window constraints.

The possibility of designing a combined mission has been considered, and rejected for several reasons. Firstly it appears that on most asteroid missions, any excess energy is best used up in decreasing the approach velocity in order to increase the observation time, rather than in setting a new trajectory to a second target. Secondly, the majority of asteroids have a negligible gravitational field, and therefore their field cannot be used to introduce deliberate perturbations (so-called gravity swinging), in order to achieve a combined mission, as has been suggested for Mars-Venus missions for example. Thirdly, there appears to be no appreciable grouping of the asteroids in a predictable manner, enabling the spacecraft to pass by several asteroids without alteration of its trajectory. A search for such grouping among all the asteroids whose orbits are known has been conducted on IITRI's 7090 computer but with negative results, although short lived grouping of a random nature, was noticed.[15]

A summary of some guidance and control calculations for the four targets considered has been given. Guidance, acquisition, and target encounter procedure, are felt to be prime considerations in the design of an asteroid mission because of the small size and high relative velocity of these bodies.

Three hypothetical launch vehicles are considered, the first having a capability of putting a 500-750 lb. package to escape, the second 2000-3000 lbs. and the third 6000-7000 lbs. These will be designated Vehicles A, B, and C respectively in the tables throughout this report. These appear to cover the range required by the missions adequately, without resorting to the use of more futuristic vehicles. For many missions, it is essential to postulate the addition of a high performance stage on top of the stipulated launch vehicle in order to deliver significant payloads. This stage is assumed to have an I_{SP} of 440, and to be compatible with the lower stages. Its structure factor is taken to be 10 per cent.

In all cases where an extra stage is included in the calculations, it is assumed that the basic launch vehicle puts this stage into a 300 N. mile parking orbit. It should be pointed out that the figures quoted for very small payloads represent a small fraction of the launch vehicle weight, and hence are extremely sensitive to vehicle performance.

The weights quoted throughout this report are largely derived from state of the art figures. If one assumes an overall improvement of say a factor of two, then many of the missions that appear to be marginal become very real possibilities.

4.2 An Asteroid Fly-Through Mission

Before treating any missions to the larger bodies, the potentialities of a simple spacecraft flying through the belt will be discussed. Such a spacecraft is attractive because of its inherent lack of terminal or mid-course propulsion, resulting in a more efficient allocation of the scientific payload. In addition, such a mission does not suffer from having any launch window constraints.

The capabilities of a spacecraft flying through the asteroid belt, without being directed at any particular target are necessarily somewhat limited, but for this very reason may present the highest probability of success of all the mission configurations. Such a mission would provide an admirable opportunity for examining the interplanetary magnetic field out to 3.5 AU (or more), and in particular detect the presence of any turbulence in the field. The primary reason for such a mission however, would be to study the mass distribution in the belt, and hence enable a spacecraft collision cross-section to be derived for the first time. In this respect one difficulty arises immediately, namely how large does the particle detector have to be in order to record a statistically meaningful number of events?

4.2.1 The Particle Density

The almost complete lack of data on the distribution of small particles in the region 2 to 3.5 AU makes any attempt to estimate the particle density and collision probability in that region extremely difficult to jjstify. By making a number of sweeping assumptions however, we can try to arrive, within one or two orders of magnitude, at a figure for the particle density. These assumptions are:

1. The total mass of the asteroids, as estimated by Kuiper and others at between 0.0004 and .001 of earth's mass, i.e., 2 to 6 x 10^{24} gms; let us assume the upper limit.

2. At any instant the asteroid density is uniform, constant, and the total mass is contained in an oblate toroid extending from 2 AU to 3.5 AU with a thickness of 1.2 AU which corresponds approximately to orbital inclinations between + 10° to - 10° to the ecliptic.

3. The asteroid belt contains particles of average density approximately the same as that of the stony meteorites, i.e., 3 gm/cc.

Using these figures the mass/cubic kilometer in the belt is 0.06 gms.

If this is totally invested in particles of 1 μ radius, the number of particles per km^3 is 6×10^9, or 6 per cubic meter.

The particle density for different sizes of particles can be similarly calculated, e. g.

1 μ radius	6×10^9 per km^3
10 μ radius	6×10^6 per km^3
100 μ radius	6×10^3 per km^3
1 mm radius	6 per km^3
1 cm radius	6×10^{-3} per km^3

From these figures the number of encounters anticipated by a given spacecraft may be calculated.

The total mass encountered, ignoring statistical variations, is the product of the mass density and the effective volume swept out by the spacecraft. It is now necessary to make a further assumption about the spacecraft trajectory. Let us assume that it travels radially outwards from 2 to 3.5 AU, and presents one square meter of frontal surface. The volume swept out would be 2.25×10^{11} cubic meters and the mass encountered, 13.5 gms.

This rudimentary calculation ignores the fact that the asteroids are moving with a mean orbital velocity of approximately 20 km/sec, which would cause the intercepted mass to increase by a factor of three or four for a spacecraft velocity of 7 km/sec, i. e., the total mass encountered per square meter of frontal area would be approximately 40 gms, and total momentum about 800 kg. meter/sec. Assuming for the moment that the transfer of momentum is non-catastrophic, it can easily be shown that the momentum of the asteroids encountered amounts to approximately one thousandth of that of a 500 lb. spacecraft on a 100 day mission through the belt. The momentum although imparted in a preferred direction, would therefore not result in a serious trajectory perturbation. It is also to be noted that in this case, the perturbation would not be large enough to detect.

It seems apparent that even a modest sized micrometeorite counter would record a considerable number of impacts during a 100 day flight. In addition to this experiment, measurement of the scattered sunlight from the asteroidal dust by a photometric experiment, could provide a back-up system which, providing the data from the two experiments correlated, would provide convincing information on the particle size distribution. The addition of a radar experiment, to study the larger particle distribution, as previously described, would provide significant data on the entire size spectrum of particles in the belt.

The fly-through mission would provide an admirable chance to measure the interplanetary magnetic field out to 3.5 AU (or more), and in particular detect the presence of any turbulence in the field. [16]

The communications equipment from such a fly-through spacecraft need not be elaborate. At 3 AU for example, a spacecraft carrying a 25 db antenna could transmit 10 bits/sec for a power of 4 watts. Figure 7 shows the relationship between range, transmitter power, and bit rate, based on an assumed 25 db antenna, working at 'S' band, and an Earth based 85 ft. antenna. If the 210 ft. antennas proposed for D. S. I. F. were used, the required power would be reduced by a factor of six. A typical payload for a fly-through mission is shown in Table 9.

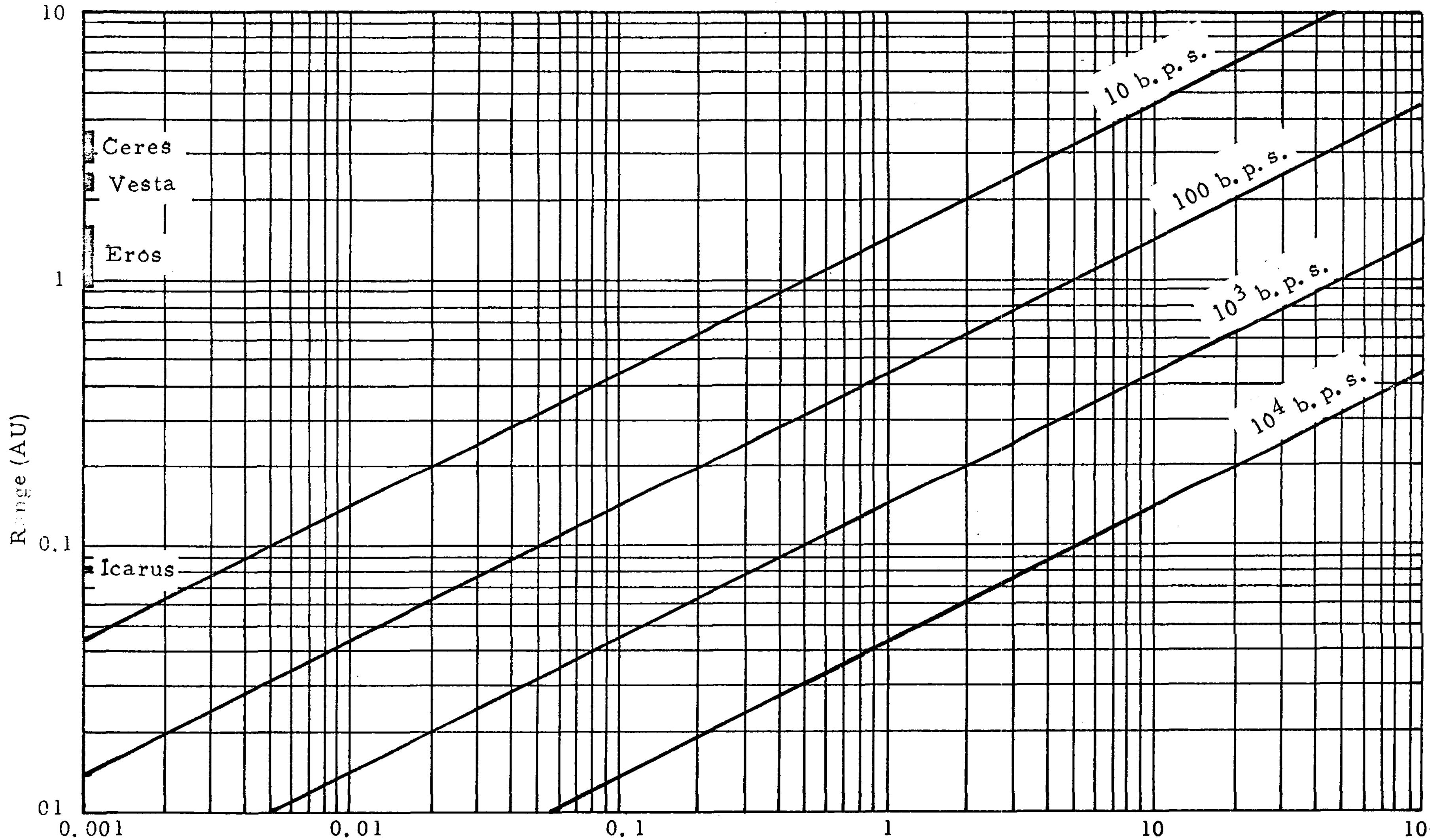

Fig. 7 TRANSMITTER POWER (WATTS) AS A FUNCTION OF RANGE AND INFORMATION RATE FOR ASTEROID MISSIONS

The 300 lb. payload suggested could be delivered to 4 AU by Vehicle C within 600 days. By postulating an additional final stage (that makes full use of the launch vehicles' capability, Vehicle B could deliver the payload in 300-400 days. There are no launch window restrictions, since the mission is not directed at any specific target body.

Table 9

PAYLOAD BREAKDOWN FOR A FLY-THRU MISSION

		Weight
1.	Radar Experiment Photometer Experiment Magnetometer	40
2.	Transmitter (10 W at 'S' Band) Data processing and storage	25
3.	Antenna (25 db)	10
4.	Attitude Control	30
5.	Power Supply (150 W isotopic)	150
	Batteries	30
6.	Structure and Meteorite shield (Shielded area = 100 square feet, probability of no penetration 90%)	35
		320 lbs.

4.3 Mission to Eros

Six possible target asteroids are tabulated in Table 10, the six being the four largest asteroids plus two smaller asteroids that have close approaches to Earth.

The first to be considered for a possible mission to Eros, primarily because it is an interesting body from a scientific viewpoint, and secondly because its close approach to Earth makes it possible to launch comparatively low energy missions.

Eros has several notable features which make it an attractive target for an asteroid mission. Of all the known asteroids it is the most likely to be a collision fragment, since its light curve displays variations of nearly 1.5 magnitudes, with little or no change in color. Indeed its light curve is so spectacular that it has been suggested that Eros is a double asteroid, the two bodies rotating around the common center of mass. If one does assume that Eros is an irregularly shaped body, the observations indicate[17] that its dimensions are approximately 22 km by 6 km.

At closest approach, this body is only 23×10^6 km away from the Earth, thus making short flight times (100-150 day) possible without resorting to high energy missions. Restraints are imposed however, by the need to perform highly accurate mid-course and terminal maneuvers.

The first objective of a mission to Eros would be to examine its gross physical features, and verify that it is indeed a collision fragment. The shape of the body can be ascertained with even the crudest of television experiments (for example a ten by ten matrix of photodetectors in the image

Table 10

CHARACTERISTICS OF SIX NOTABLE ASTEROIDS

	Diameter (km)	Apparent Magnitude	Perihelion	Aphelion	Orbital Period	Orbital Inclination
Ceres	770	3.7	2.56	2.98	4.6	10
Pallas	490	4.4	2.12	3.42	4.6	34.8
Juno	193	5.74	1.98	3.76	4.3	13.0
Vesta	386	3.5	2.15	2.57	3.6	7.1
Eros	22 x 6	9 - 10.4	1.13	1.78	1.76	10.8
Icarus	1.5	18	0.19	1.97	1.12	23.0

plane of a small telescope). A more sophisticated system is certainly necessary to provide information on the gross surface features and dust layer. A system similar to the Ranger TV system but using only one camera should be adequate.

In the section describing possible experiments for an asteroid mission, the similarity between the asteroid lander and the Surveyor soft lunar lander has been mentioned. The surface features of the moon and the larger asteroids in fact appear to have much in common. It is suggested that for Eros, once the spacecraft is committed to making a terminal maneuver which reduces VHP to zero, there is every reason go to to the whole way and design the mission for a soft lander since gravitational attraction will cause an eventual landing anyway, and measurement by the radar altimeter of the spacecraft's rate of descent is probably the easiest method of measuring the asteroid's mass.

For Eros, if one assumes the dimensions are as stated, and the average density is 3 gm/cc, the escape velocity is 9 meters/sec. Using Surveyor as an example again, its velocity at impact is planned to be 4 m/sec, and so a similar landing on Eros would entail the removal of only 5 m/sec or so. One problem unique to Eros that ought to be pointed out however, is that its shape is thought to be elongated 22 km by 6 km, and its period of rotation only 5-1/2 hours, which means that the extremities of Eros have a velocity due to rotation of 3.5 m/sec. This makes the landing procedure more difficult but not impossible.

Figures 8, 9, and 10 show the fraction of the mass in 300 N. mile parking orbit that can be sent to Eros in 75, 100 and 125 days respectively, by using an extra high performance stage for injection into the transfer conic. The fraction left after all relative velocity between spacecraft and target has been removed is indicated by the curve marked "final payload". The figures are plotted this way in order to show the effect of the combined maneuvers on the total payload. Table 11 gives specific examples of the payload capabilities of the postulated vehicles with and without the extra kick stage.

The payload breakdown for an Eros mission is given in Table 12. Propulsion for the terminal maneuver has not been included so as to make the table compatible with the "final payload" curve of Figures 8, 9, and 10.

As previously mentioned, the very low figures shown for launch vehicles with no added stage are unreliable since a small variation in the structure factor allowed could cause them to drop to zero.

It can be seen that Vehicle B plus an added stage is capable of hard landing the entire experimental package described on Eros in 125 days with an ample margin to spare. A soft lander with this launch vehicle would be extremely marginal. Vehicle C displays ample capability for a 125 day mission, provided the added stage is used. In this instance, the added stage need not be the high performance stage previously described, even a modest upper stage, with an I_{SP} of 350 would enable Vehicle C to land 1000 lbs. on Eros in 125 days.

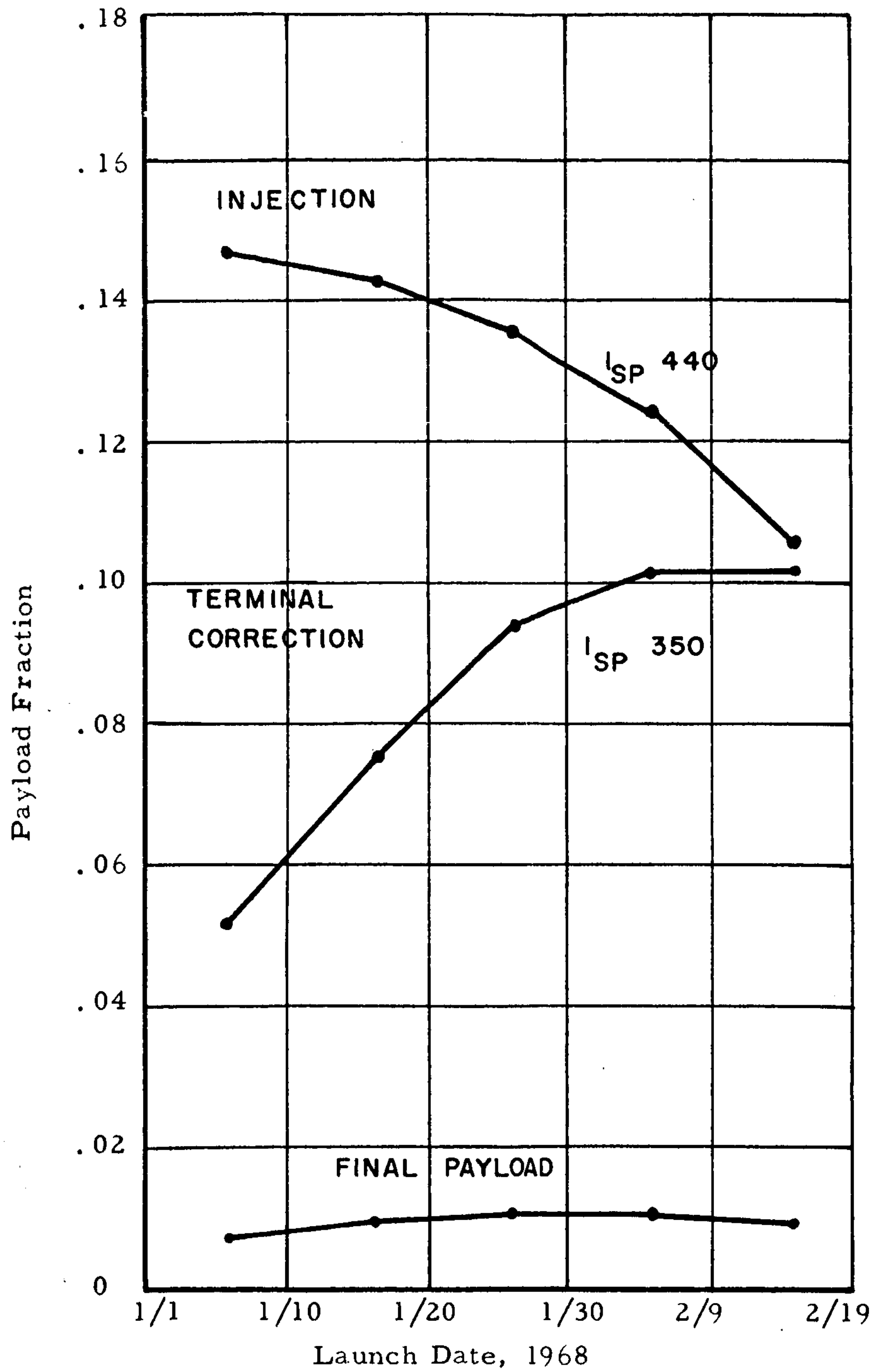

Fig. 8 PAYLOAD FRACTION AVAILABLE FOR A 75 DAY FLIGHT TO EROS, SHOWING

a) Fraction of payload remaining after injection from 300 N. M. parking orbit

b) Fraction of injected payload remaining after terminal maneuver

c) Final payload expressed as a fraction of mass in parking orbit.

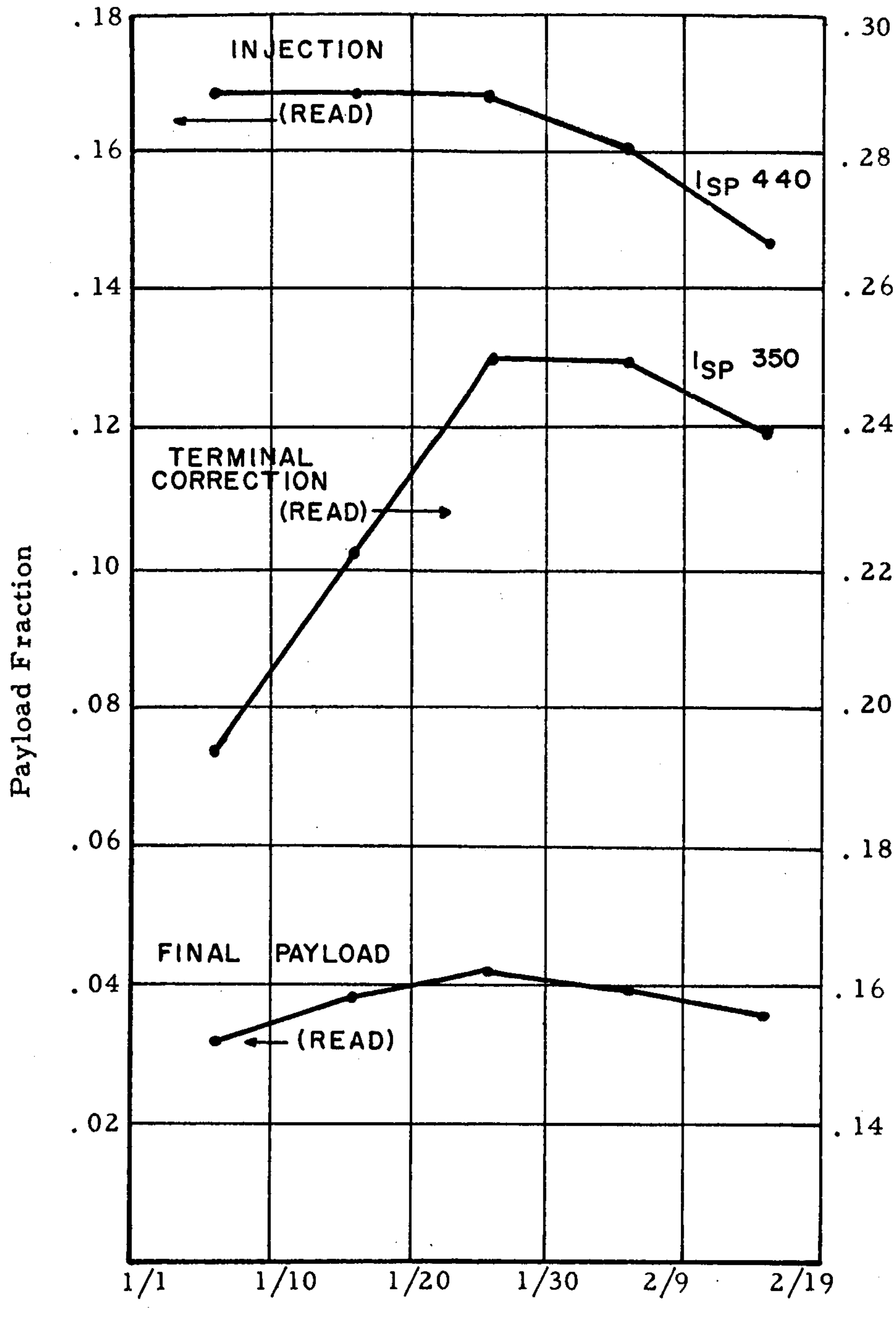

Fig. 9 PAYLOAD FRACTION AVAILABLE FOR A 100 DAY FLIGHT TO EROS, SHOWING

a) Fraction of payload remaining after injection from 300 N. M. parking orbit
b) Fraction of injected payload remaining after terminal maneuver
c) Final payload expressed as a fraction of mass in parking orbit

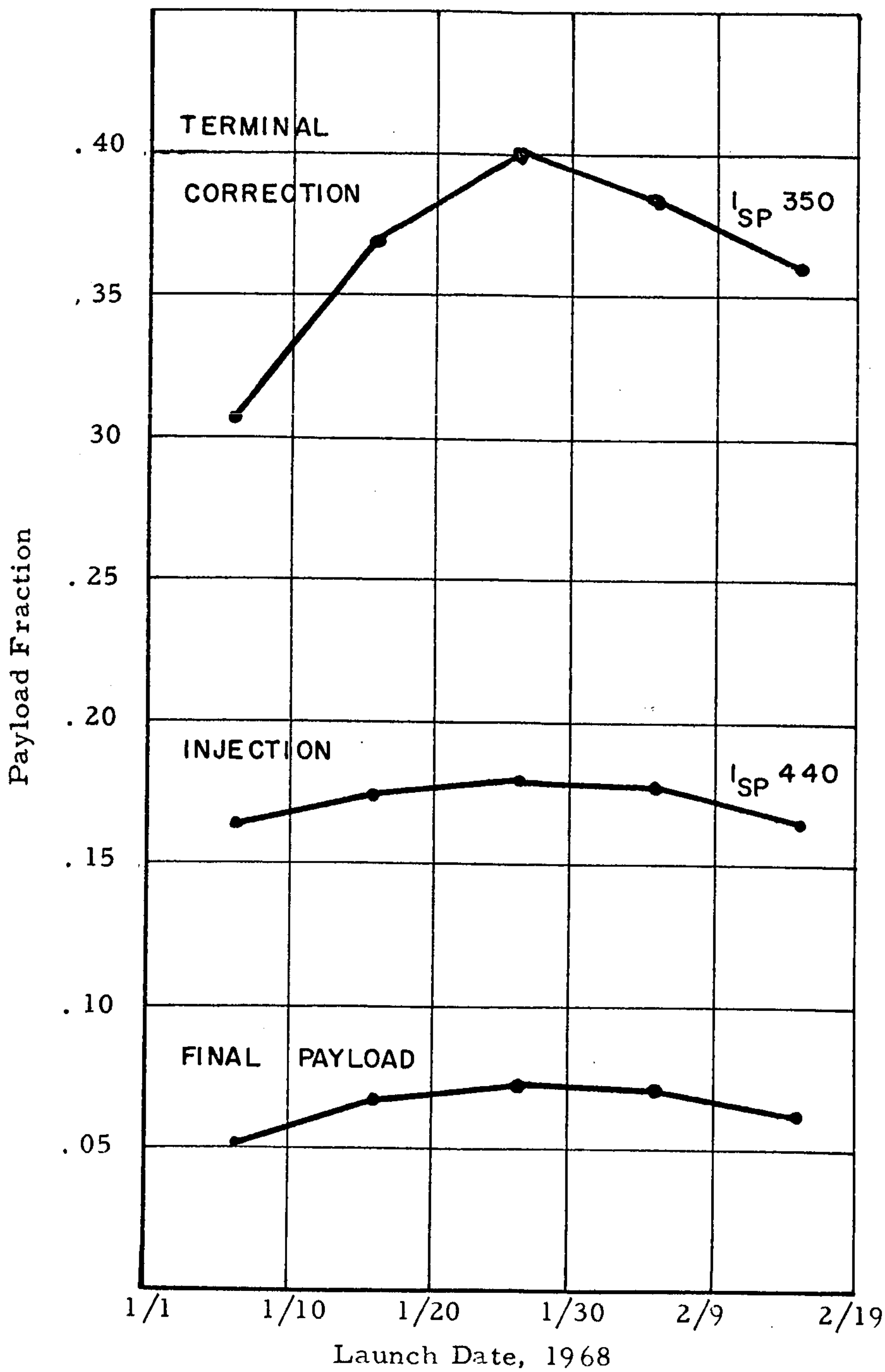

Fig. 10 PAYLOAD FRACTION AVAILABLE FOR A 125 DAY FLIGHT TO EROS, SHOWING

a) Fraction of payload remaining after injection from 300 N. M. parking orbit

b) Fraction of injected payload remaining after terminal maneuver

c) Final payload expressed as a fraction of mass in parking orbit.

Table 11

POSSIBLE PAYLOADS AVAILABLE FOR EROS MISSIONS
(30 DAY LAUNCH WINDOW)

Vehicle	Payload after Terminal Maneuver		
	75 days	100 days	125 days
Vehicle A	---	---	---
Vehicle B	---	---	25
Vehicle C	---	---	60
Vehicle A + High Performance Stage $I_{SP} = 440$	50	250	400
Vehicle B + High Performance Stage $I_{SP} = 440$	100	400	625
Vehicle C + High Performance Stage $I_{SP} = 440$	300	1250	2100

Table 12

PAYLOAD BREAKDOWN FOR AN ASTEROID FLY-BY MISSION

		Weight
1.	All experiments except seismic and x-ray analysis	80
2.	Transmitter (20 W at 'S' band)	15
	Data processing, and encoder	25
	Data storage (thermoplastic)	25
3.	Antenna (25 db)	10
4.	Attitude control	30
5.	Mid-Course propulsion	35
6.	Power supply (200 W isotopic)	200
	Batteries	40
7.	Structure (17%)	75
8.	Meteorite bumper shield 100 square ft. 90% probability of no penetration	15
		550 lbs.

(Weight estimates largely extrapolated from Mariner, Surveyor and Voyager data)

It should be noted that in the case of Eros extending the flight time beyond 125 days does not decrease VHL except for one narrow launch window in 1967, when for 5 days or so a 175 day mission would require less than 5 km/sec. However a strong argument for using the largest flight time available lies in the fact that the value of VHP decreases sharply as the flight time increases. A table of mission parameters illustrating this is given in Table 13. (For completeness, a conversion graph of VHL against "Ideal Velocity" is also included at the end of this report. See Figure 15.)

Flight Time	VHL (km/sec)	Asymptotic Approach velocity at encounter (km/sec)	Communication Distance (AU)	Launch Date
75 days	8.4	6.5	0.32	1/6/68
100 days	7.8	3.6	0.5	1/26/68
125 days	7.5	2.4	0.67	1/26/68
150 days	7.1	1.8	0.98	2/5/68
175 days	7.2	1.3	1.14	1/26/68
200 days	7.1	1.0	1.41	1/26/68
225 days	7.1	0.9	1.69	1/26/68
250 days	7.0	0.9	1.96	1/26/68

Table 13 OPTIMUM LAUNCHES FOR EROS

4.4 Mission to Ceres

Ceres is the largest of the known asteroids and is thought to account for approximately 1/3 of the total mass of the asteroid belt. It orbits between 2.56 and 2.98 AU with a period of 4.6 years. Kuiper[18] has pointed out that any body formed, and having a nearly circular orbit at less than 4 AU, whilst Jupiter was in the protoplanet stage, would be constrained to remain thereafter inside that limit. This cannot of course be interpreted as meaning that all bodies inside 4 AU must have originated there, but it does indicate that to gather information on the origin of the asteroid belt, one would limit any mission to bodies such as Ceres, which orbit inside that limit. In an earlier paper[19], Kuiper argues that any body the size of Ceres must have been created by an accretion process. Urey[20] also pays considerable attention to the thermal history of a body the size of Ceres.

Ceres is, undoubtedly, the most interesting of the distant asteroids, and would seem to be a worthwhile objective.

A soft lander seems essential, if one is to answer the questions about the internal structure, remaining radioactivity, and composition of Ceres. Such a spacecraft would contain all the experiments listed in the earlier section. A Ceres fly-by, however, could measure the following:

- Size
- Temperature
- Magnetic field, if any
- Rotation rate
- Surface characteristics

which would represent a vast increase over our present knowledge.

The approach velocities for missions to Ceres are in general higher than those for missions to Eros. Nevertheless, it does not appear essential to incorporate terminal propulsion in order to elongate the observation time during fly-by as was the case with Eros. Refering to Table 14, the value of VHP for a 350 day flight is given as 6.6 km/sec. If 10,000 km is taken as a reasonable miss distance, (Mariner 2 was 30,000 km), then the spacecraft's line of sight to the target body would turn through 60° in approximately 30 minutes, and the observation distance would not exceed 11,500 kms.

However, as was pointed out in the previous paragraph, there are many questions such as the chemical nature of the body, surface erosion, internal structure, possible radioactivity, presence of organic compounds, which can only be answered by experiments performed from the surface of the asteroid. As was the case with Eros, the difficulty in landing on Ceres is not overcoming the gravitational attraction, but reducing VHP to near zero in a terminal maneuver, before initiating the landing procedure. VHP for a 350 flight to Ceres is 6.6 km/sec, and the escape velocity for the asteroid is of the order 0.8 km/sec. Assuming that the terminal propulsion system performs the actual landing maneuver as well, its total capability then needs to be at least 7.4 km/sec. The payload for a sophisticated Ceres lander would be designed to perform the following functions:

a) measure surface gravity
b) measure surface and sub-surface temperature
c) study soil composition
d) televise the immediate vicinity
e) detect the presence of organic compounds

Table 14

OPTIMUM LAUNCHES FOR CERES

Flight Time, days	VHL (km/sec)	Asymptotic approach velocity at encounter (km/sec)	Communication Distance (AU)	Launch Date
200 days	11.7	17.7	2.74	2/18/73
250 days	8.4	10.8	3.31	1/16/68
300 days	7.3	8.0	3.72	1/16/68
350 days	6.9	6.6	3.8	1/16/68

f) detect the extent of natural radioactivity

g) measure the trapped magnetic field, if any

h) detect any natural seismic activity, and perform seismic sounding experiments using either natural or artificial excitation.

i) detect micrometeorite impacts

The electrical power required to actuate all these experiments, and transmit the data back from Ceres would be considerable. From Figure 7 it can be seen that an information rate of 100 b. p. s. would require a transmitted power of between 50 and 70 watts. The only economical solution to this problem is to limit the experimental data gathered per day, and use large data stores on board, storing say 10^8 or 10^9 bits of experimental and engineering data. The thermoplastic storage technique proposed for Voyager (Mars) stores 10^9 bits, consumes 25w, and weighs only 22 lbs., and thus appears ideal for this purpose. The lander would also have to incorporate a fairly versatile preprogrammed computer for commanding the landing, deploying, and transmission operations, since Earth based commands would suffer a 30 minute delay in reaching the spacecraft, and would therefore be of very limited use.

Figure 11 shows that the optimum launches for Ceres missions are all centered about 1/16/68 for the flight times shown. In common with all the trajectories in this report, the values of VHL were computed from 1964 to 1974, and the period of time containing the lowest minimum selected. A list of the other parameters associated with these missions is given in Table 14, and the payload capabilities of various launch vehicles in Table 15.

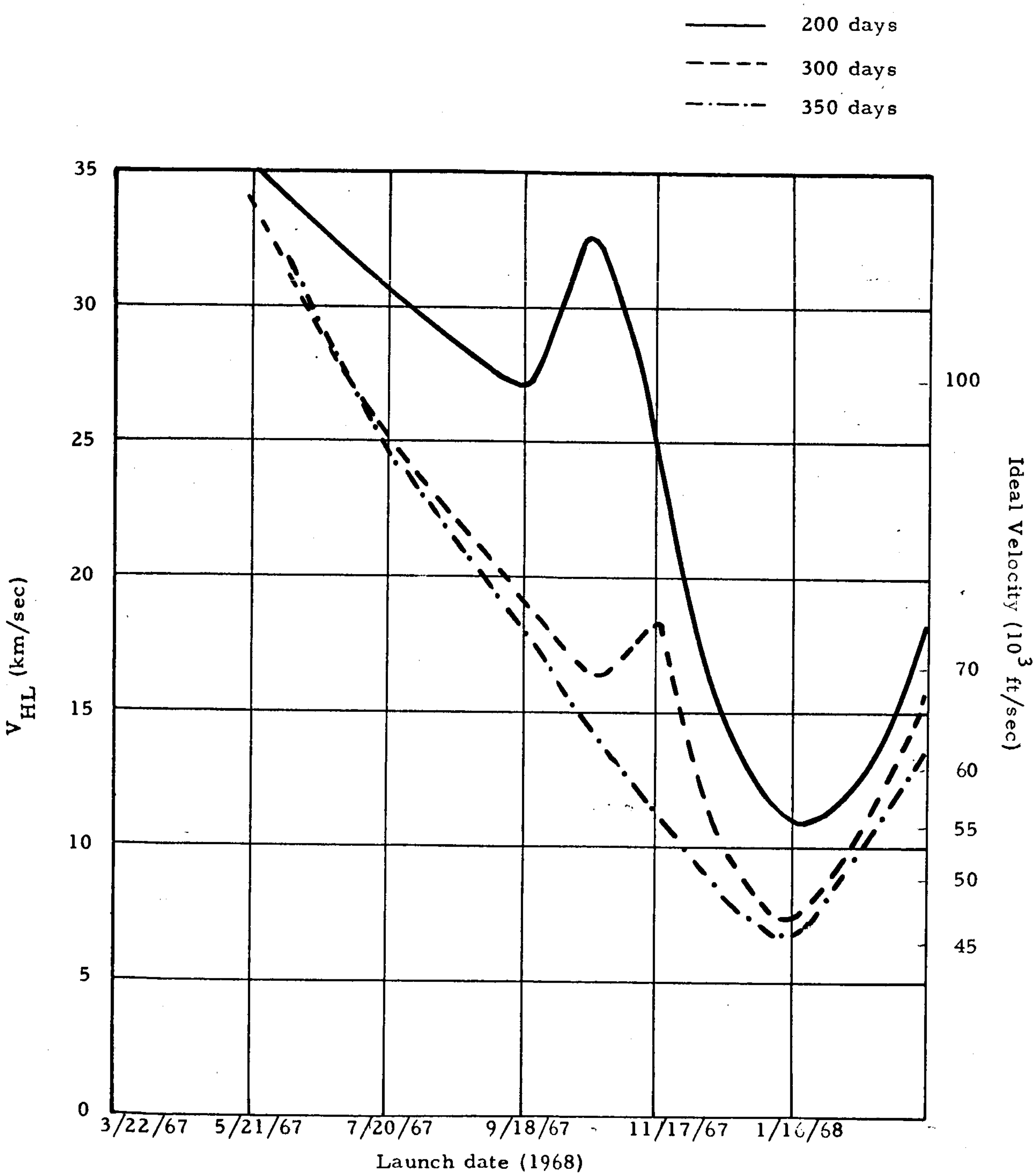

Fig. 11 MISSIONS TO CERES

Table 15

POSSIBLE PAYLOADS AVAILABLE FOR CERES MISSIONS

(30 DAY LAUNCH WINDOW)

Vehicle	Fly-By			Soft Lander		
	250	300	350 days	250	300	350 days
Vehicle A	---	---	---	---	---	---
Vehicle B	---	---	---	---	---	---
Vehicle C	---	---	400	---	---	---
Vehicle A + High Performance Stage $I_{SP} = 440$	230	800	1000	---	50	140
Vehicle B + High Performance Stage $I_{SP} = 440$	450	1300	1650	20	100	200
Vehicle C + High Performance Stage $I_{SP} = 440$	1500	4300	5500	80	300	700

(The weights shown are those of the spacecraft after the propulsive system has been allowed for.)

From this latter table it can be seen that with a suitable upper stage even Vehicle A is capable of delivering a 1000 lb. fly-by to Ceres in under a year. The weights shown for the soft landers have been based on the worst combination of VHL and VHP during a 30 day period centered about the minimum.

The 680 lb. lander delivered by Vehicle C plus a kick stage is marginally sufficient to contain all the experiments listed earlier, together with a slightly increased power supply.

4.5 Mission to Icarus

Icarus is a comparatively small asteroid (diameter 1.4 km), with a cometary orbit which brings it within 4-1/2 million miles of the Earth, and 0.19 AU of the Sun. Its close approach to Earth makes it particularly attractive as a potential target body. Icarus is also non-typical of the asteroids because of its extreme thermal cycling during orbit, ranging from 500° C at perihelion to below zero at aphelion. The effect of this environment on the surface of Icarus would be of considerable interest from a scientific point of view.

Unfortunately, Icarus has a high inclination, (23°) to the Ecliptic which has the effect of allowing very short launch windows from Earth, and high values of VHP which, coupled with its small size could make target acquisition and encounter a difficult procedure. A table of mission parameters, for flight times of 50, 75 and 100 days is given in Table 16, and a graph of VHL against launch date in Figures 12 and 13. It can be seen that even a 10 day launch window increases the value of VHL significantly. For example, a 100 day flight has a minimum VHL of just under 1 km/sec. Expanding the launch window to ten days increases VHL to 1.5 km/sec and for 30 days, VHL becomes 3.3 km/sec.

Icarus is an exceptional case in that the minima for the trajectories shown in Figure 12 lies about 20 days apart. Therefore, if instead of stipulating a constant flight time one allows it to vary from say 50 days to 100 days, the launch window can be opened to well over 30 days for values of VHL under 1.7 km/sec. In this case the values of VHL are indicated by the envelope containing all the minima in Figure 12.

Table 16

OPTIMUM LAUNCHES TO ICARUS

Flight Time, days	VHL (km/sec)	Asymptotic approach velocity at encounter (km/sec)	Communication Distance (AU)	Launch Date
100 days	1.0	28.4	0.04	3/11/68
75 days	1.2	28.5	.05	4/2/68
50 days	1.6	29.2	0.04	2/26/68

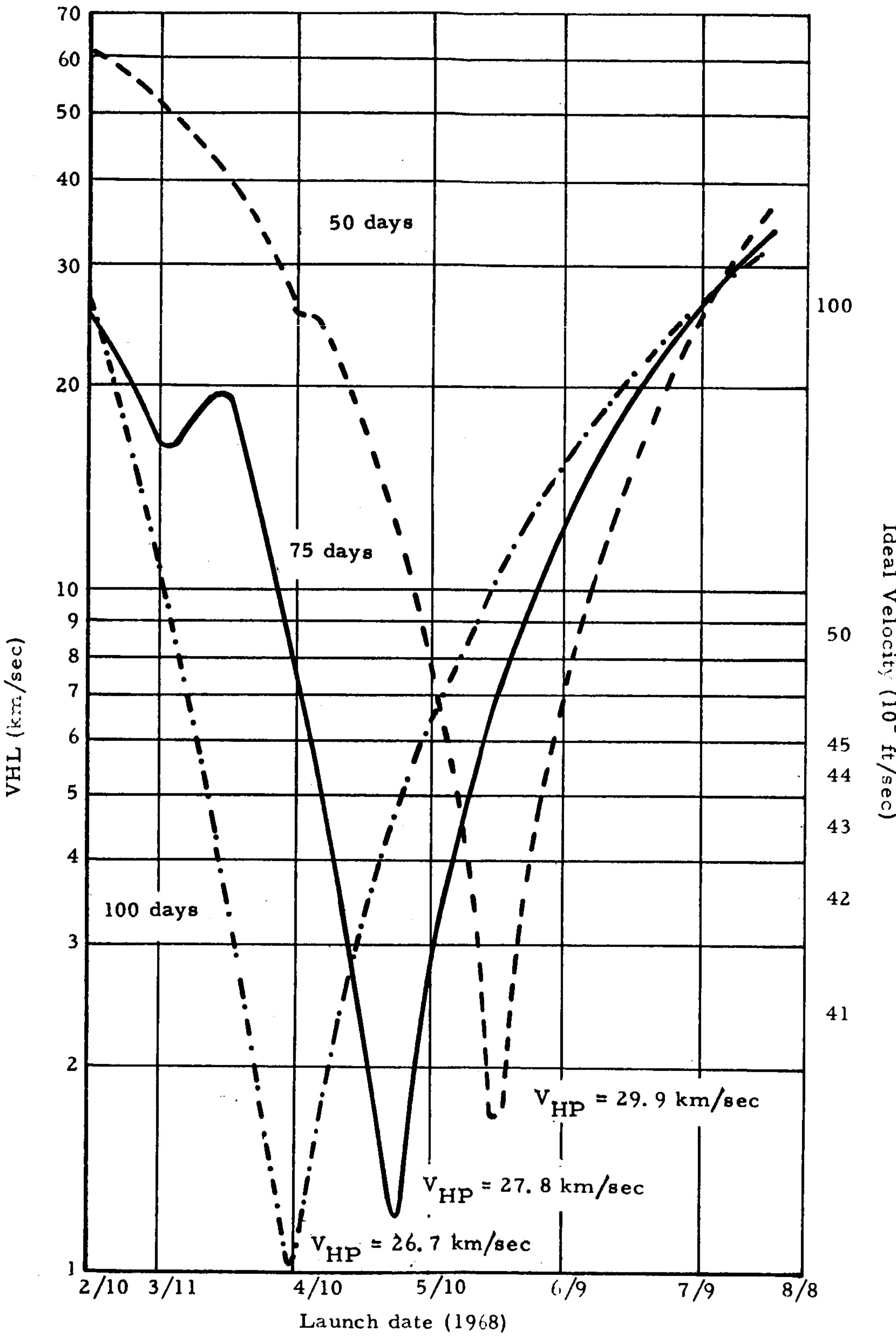

Fig. 12 MISSIONS TO ICARUS

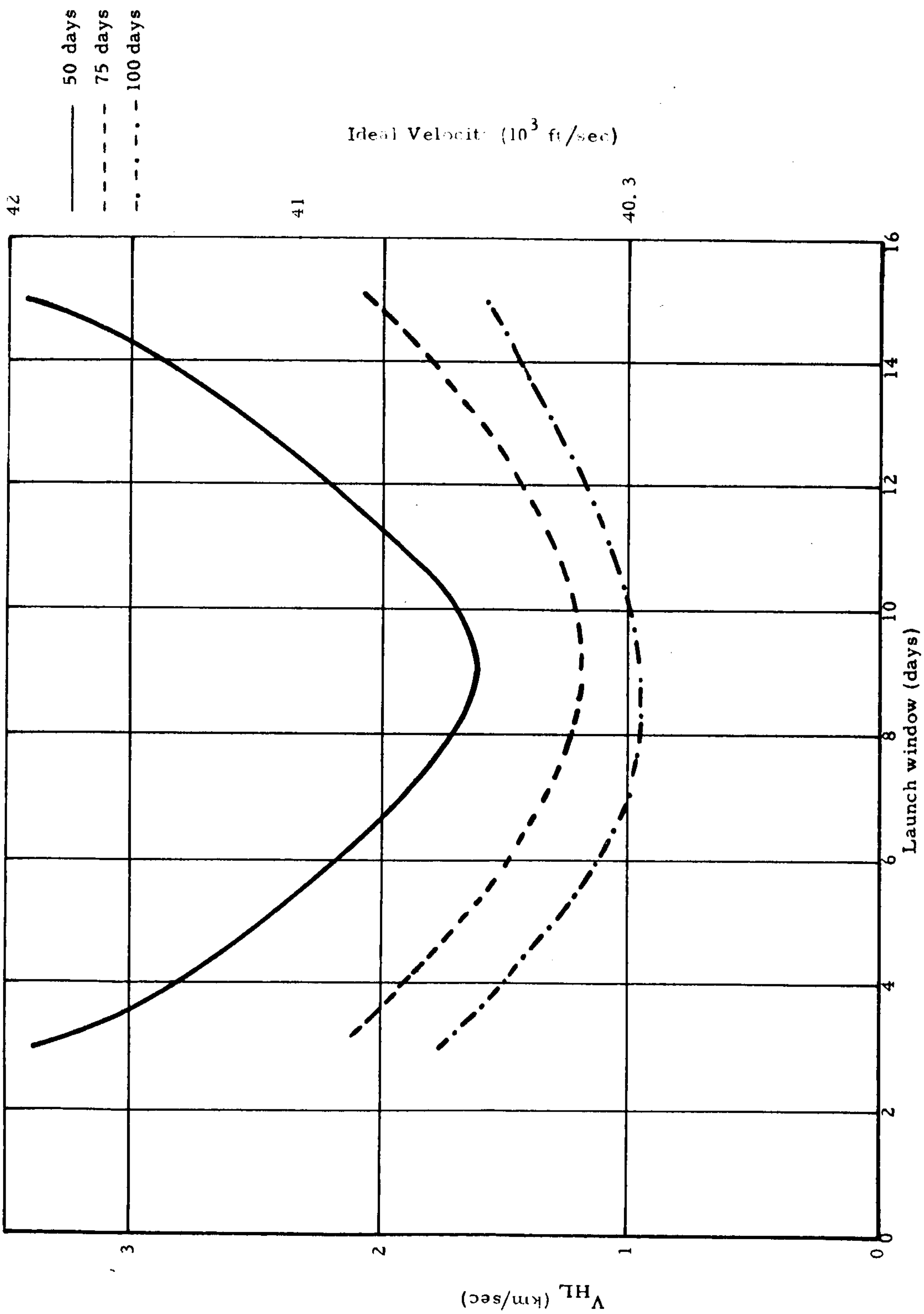

Fig. 13 ICARUS LAUNCH WINDOW

The saving in payload by adopting this approach is considerable, and would certainly outweigh any advantages obtained by predetermining the flight time.

No matter what flight time is chosen, between the limits of 50 and 100 days, if the minimum energy trajectory for that flight time is used, corresponding to a flight in the ecliptic plane, the value of VHP at encounter will always be high, never falling below 25 km/sec. This extremely high relative velocity, coupled with the small physical size of Icarus would place severe demands on the target acquisition system, and would make experimental observation of the body almost impractical, since the time available for observation would be well under one minute even from 1000 km away. (It is debatable whether any worthwhile information could be learned about a 1.4 km body from 1000 km miss distance.)

Reduction of VHP does not appear to be a solution to the problem, since the payload penalties for even a 50% reduction are too severe. Reducing VHP to 15 km/sec for example means that propulsion takes up 98% of the available payload.

Various authors have suggested the use of an asteroid, and in particular Icarus as a stable platform from which to observe the Sun and parts of the Solar System. The propulsion difficulties outlined in the preceding remarks illustrate the impracticability, at this time, of such a project.

A mission to Icarus would therefore depend on the development of a sophisticated target acquisition system, high resolution experiments that could observe the asteroid from a thousand radii away, and a sound guidance and central system. Landing on the asteroid is definitely not an economical proposition using chemical propulsion. Table 17 shows the payload capabilities of several launch vehicle combinations for the fixed time of flight missions and the variable flight time mission. For the latter, even Vehicle A is capable of delivering a 600 lb. fly-by to Icarus. The advantages of using the variable flight time mode are obvious.

Table 17

POSSIBLE PAYLOADS AVAILABLE FOR ICARUS MISSIONS

(30 DAY LAUNCH WINDOW)

Vehicle	Payload (lbs.) for Given Flight Time			
	50 days	75 days	100 days	Variable flight time 50 - 100 days
Vehicle A	275	150	---	600
Vehicle B	1, 600	1, 000	---	2, 800
Vehicle C	3, 200	3, 000	400	5, 500
Vehicle A + High Performance Stage $I_{SP} = 440$	1, 600	1, 400	875	3, 900
Vehicle B + High Performance Stage $I_{SP} = 440$	3, 000	2, 500	1, 500	6, 600
Vehicle C = High Performance Stage $I_{SP} = 440$	10, 000	8, 400	5, 200	23, 400

4.6 Missions to Vesta

Many of the remarks applied earlier to Ceres missions can also be applied to Vesta. The body is the third largest of the asteroids, being approximately 380 kms in diameter. It is however an easier target to reach from Earth, since its orbital inclination is only 7° and it is considerably closer. As with all the other asteroids, very little is known about Vesta. Its one peculiarity is that its albedo is extremely high (0.25), otherwise it is a typical asteroid. It is included in this study not only because the same questions as can be applied to the largest body, Ceres, can also be applied to Vesta, but also because of the four largest bodies, Vesta has the least unfavorable launch conditions (see Figure 14). Vehicle B for example can deliver an approximately 700 lb. fly-by to Vesta in 275 days (with no upper staging).

Table 18 shows the mission parameters associated with 200, 225 and 275 day flights to Vesta, and Table 10 lists the payloads (exclusive of propulsion as before) available for fly-bys and soft landers using the vehicles suggested. The contrast with the figures for Ceres is worth noting, e.g. Vehicle C can land 300 lbs. in 300 days on Ceres, or 1100 lbs. in 275 days on Vesta. Since the escape velocity of Vesta is only of the order 0.4 km/sec, the idea of landing on the asteroid and returning to Earth with a few pounds of Vesta on board becomes a real possibility, bearing in mind that either atmospheric braking or lunar landing is available for the return trip.

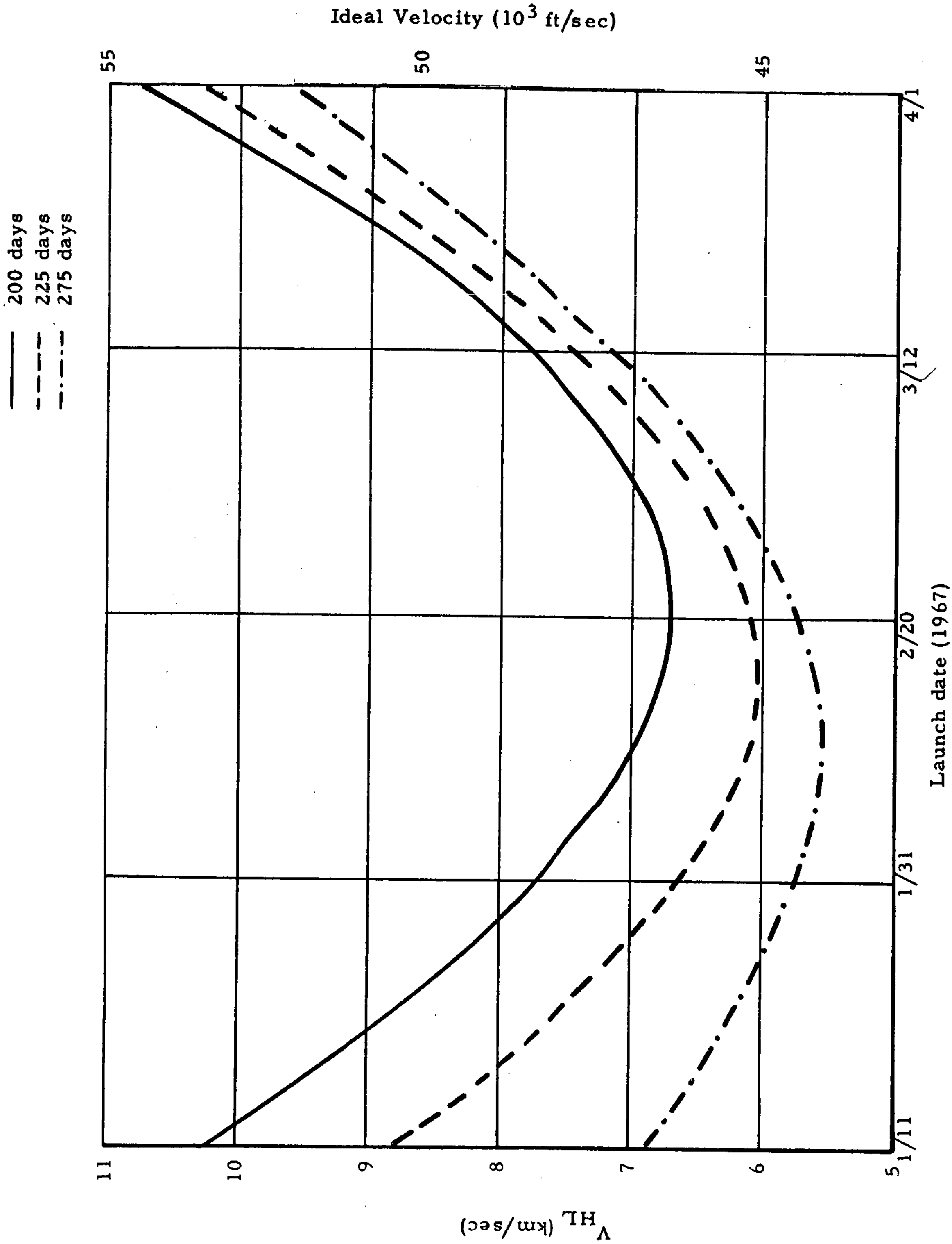

Fig. 14 MISSIONS TO VESTA

Table 18

OPTIMUM LAUNCHES TO VESTA

Flight Time (days)	VHL (km/sec)	Asymptotic Approach Velocity at Encounter VHP (km/sec)	Communication Distance (AU)	Launch Date
200	6.7	10.1	1.96	2/20/67
225	6.1	8.2	2.36	2/20/67
275	5.6	6.5	2.77	2/10/67

Table 19

POSSIBLE PAYLOADS AVAILABLE FOR VESTA MISSIONS

(30 DAY LAUNCH WINDOW)

Vehicle	Fly-By			Soft Lander		
	200 days	225 days	275 days	200 days	225 days	275 days
Vehicle A	---	---	---	---	---	---
Vehicle B	170	380	700	20	50	100
Vehicle C	550	800	1000	60	100	150
Vehicle A + High Performance Stage $I_{SP} = 440$	1100	1200	1350	125	160	200
Vehicle B + High Performance Stage $I_{SP} = 440$	1800	2000	2200	200	250	350
Vehicle C = High Performance Stage $I_{SP} = 440$	6000	6700	7300	675	900	1100

5. CONCLUSIONS AND FINAL COMMENTS

The ASC/IITRI Asteroid Mission Survey has outlined the scientific objectives of any investigation of the asteroid belt, both for a specific target and a general fly-through mission with no target. This has been followed by suggestions for experiments to achieve these objectives, and a brief description of the configuration of typical payloads, culminating in a study of the capabilities of several launch vehicles for various asteroid missions. The guidance requirements for such missions have been treated in some detail as it is felt that in many instances guidance will be a critical factor.

Due to the sparse quantity of data available covering the asteroid belt, it has been necessary to make a number of assumptions during the evaluation of these missions, and these have been stated where applicable. The most important area in which there is lack of knowledge is in estimating the collision probability between spacecraft and asteroid debris during passage through the belt. It is felt that the first missions to travel beyond 2 AU should certainly be designed to measure this parameter. For missions to nearer bodies like Eros or Icarus, the meteorite impact rate is not expected to be any higher than that experienced during the Mariner 2 flight, but this again is an assumption made from very little data.

The discussions on the capabilities of the various vehicles reveals that without an added stage, preferably high performance, their usefulness is limited. With no extra stage, Vehicle A can deliver significant payloads to one of the bodies considered, Icarus. Vehicle B however is capable of delivering a 700 lb. fly-by, or 100 lb. lander to Vesta, as well as reaching Icarus.

With the added stage, even Vehicle A is capable of reaching all four of the bodies considered with payloads ranging from 390 to 1600 lbs. Missions involving landing do not appear possible without the hypothetical extra stage, to any of the classes of target body considered.

Many of the assumptions stated in the earlier ASC/IITRI report, "Survey of Jovian Missions" are pertinent here also, and perhaps ought to be reiterated:

a) The trajectories have all been computed assuming that the spacecraft is influenced by the Sun's gravity only, and impulsive acceleration has been assumed.

b) A 30 day window has been assumed as necessary, to allow for temporary malfunctions during checkout, and adverse weather conditions. This parameter is especially critical for missions to Icarus and Eros. Any reduction in the launch window would produce significant improvement in the payloads available.

In conclusion, it is apparent from this asteroid study that exploration of both the main asteroid belt and close approach by current generation vehicles appears both feasible and practical, and indeed, the time when a return mission to a large asteroid may be planned, bringing back the first samples of asteroidal matter, may not be far off.

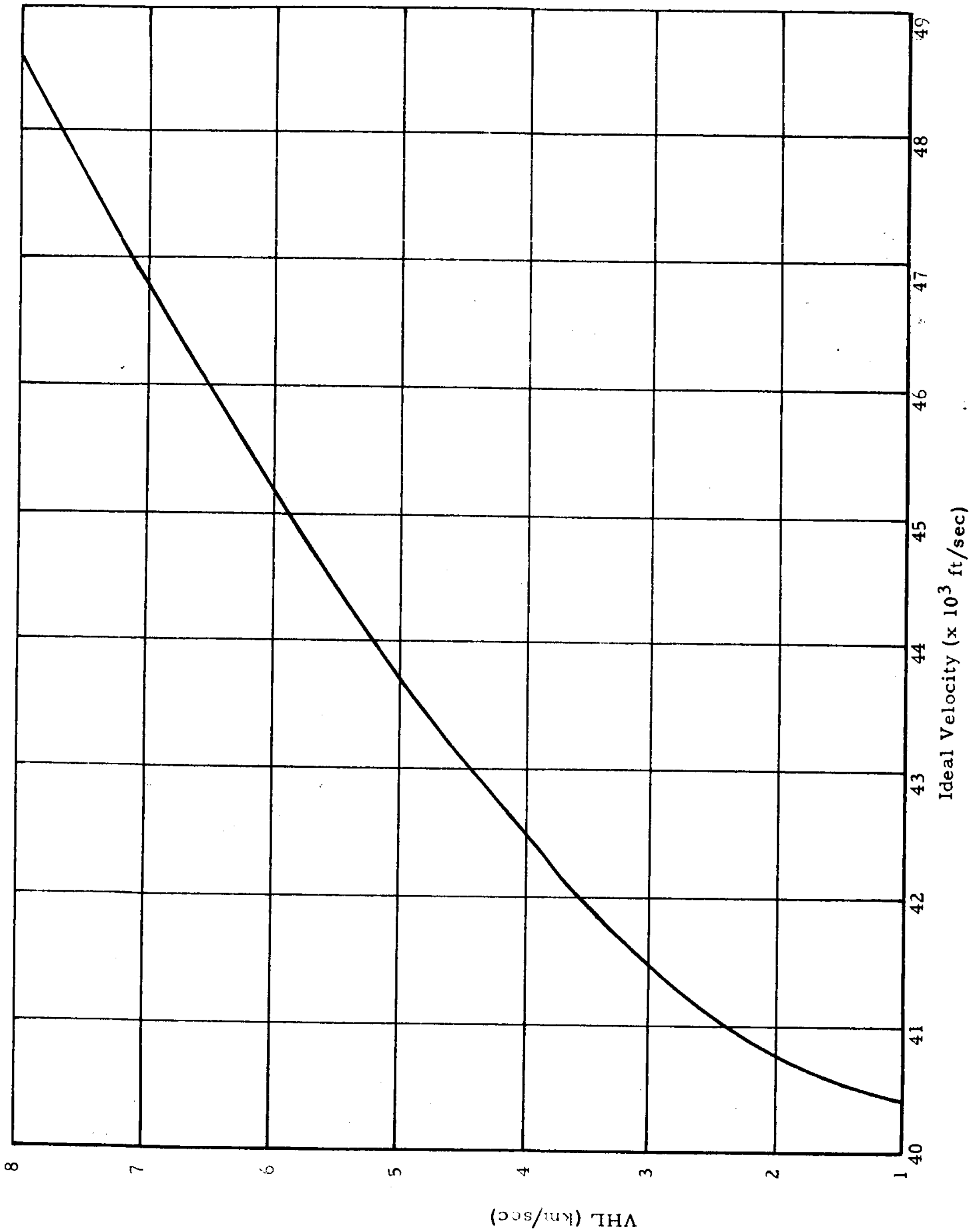

Fig. 15 THE RELATIONSHIP BETWEEN IDEAL VELOCITY AND VHL

REFERENCES

1. Alfven, H., (1954), On the Origin of the Solar System, Oxford Press.

2. Kuiper, G. P., et al, (1958), Survey of the Asteroids, Astrophysical J. Suppl. Series, Vol. 3, p. 289.

3. Brown H., The Density and Mass Distribution of Meteoritic Bodies in the Neighborhood of the Earth's Orbit, Space Research, Vol. I, Ed. H. Kallman Bijl, North Holland Publishing Company.

4. Roberts, D. L., (1963), Scientific Objectives of Deep Space Investigations, ASC/IITRI Report No. 1. 4 P2 No. 2.

5. Groenveld, I., and Kuiper, G. P., (1954), Photometric Studies of Asteroids, I. Astrophysical J. Vol. 120, p. 200.

6. Piotrowsky, S., (1953), The Collision of Asteroids, Acta. Astron. Vol. 5, p. 115-138.

7. Briggs, H. H., (1962), The Distribution of Life in the Solar System, STAR N63-10771.

8. Roberts, D. L., Private Communication.

9. Elsasser, H., (1963), The Zodiacal Light, Planets and Space Science, Vol. 11, p. 1015-1033, Pergamon Press.

10. The Feasibility of Utilizing an Isotropic Neutron Source for Compositional Analysis of Lunar or Planetary Surfaces, IITRI Proposal No. 63-875A (1963).

REFERENCES (Cont'd)

11. Wilhite, W. F., (1963), The Development of the Surveyor Gas Chromatograph, JPL TR 32-425.

12. Lehner, F. E., et al (1962), A Seismograph for Lunar Experiments, J. Geo. Res. Vol. 67, No. 12.

13. Coombs, L. C., (1963), How Much Meteoroid Shielding for Spacecraft, Space/Aeronautics.

14. Volkoff, J. J., (1963), Protection Requirements for the Resistance of Meteorite Penetration of Interplanetary Spacecraft Systems, AIAA Electric Propulsion Conference, Colorado Springs, March 1963.

15. Narin, F., (1963), Spatial Distribution of the Numbered Asteroids (Preliminary Draft) ASC/IITRI report.

16. Meyer, P., Parker, E. N., and Simpson, J. A., (1956), Phys. Rev. Vol. 104, No. 3, p. 768-783.

17. Watson, F., (1956), Between the Planets, Harvard University Press.

18. Kuiper, G. P., On the Origin of the Satellites and Trojans, Vistas in Astronomy, (Ed. by Beer), Vol. 2, Pergamon Press.

19. Kuiper, G. P., (1953), Note on the Origin of the Asteroids, Proc. N. A. S., Vol. 39, p. 1153-1161.

20. Urey, H. C., (1956), Diamonds, Meteorites and the Origin of the Solar System, Astrophysics J., Vol. 124.

REFERENCES (Cont'd)

21. Evans, J. V., Radar Echo Studies of the Moon, in Physics and Astronomy of the Moon, Academic Press, New York.

22. Colomb, G., and Fiocco, G., (1963), Optical Radar and Meteoric Fragmentation, Special Report No. 139, Smithsonian Institution, Astrophysical Observatory.

APPENDIX I

OPTICAL TRACKING OF PASSIVE BALLOONS

It has been suggested that the distribution of mass in the asteroid belt be investigated by sending a series of passive balloon type probes into the belt, noting the deflections in the balloon trajectories, and hence calculating the momentum transfer between balloon and asteroidal dust.

The tracking function can only be accomplished by radar or optical techniques if the probe is to be passive. The former alternative can be immediately discounted on account of the unrealistic power required to track even a large balloon. (A balloon 10 km diameter for example would require many megawatts for tracking to 3 AU.)

There are a number of ways of arriving at an estimate of the tracking capability of existing telescopes. The following elementary calculation shows that even if one neglects the 'noise' contribution from the atmosphere and the Earth's dust belt, optical tracking to 3 AU calls for extremely large balloons.

The Solar Constant = 1.38 kw/meter^2, therefore at 3 AU the solar flux is 153 w/meter^2.

If we assume 100 per cent specular reflection for small angles of incidence, a fraction

$$\frac{r^2}{R^2} A_T = \frac{A_T A_B}{\pi R^2}$$

is returned to the telescope.

Where A_B = cross-sectional area of the balloon (radius r) and A_T = the telescope aperture area, the incident energy = 153 A_B w/meter^2. Therefore

$$\text{reflected energy} = \frac{153.\ A_T A_B}{\pi R^2} \ \text{w/meter}^2$$

$$= A_T \cdot A_B \times 1.3 \times 10^{-23} \ \text{w/meter}^2$$

Let us assume the use of a 200'' telescope, A_T 19 meter^2.

Energy collected by the telescope = $A_B \times 10^{-20}$ w. Let us now assume that 1 watt is equivalent to 27.8×10^{17} photons/sec (the value for 5550 Å). The 200'' instrument is quoted as being able to detect objects of 23rd apparent visual magnitude with ideal seeing conditions. 20th magnitude is equivalent to 3.3×10^{-14} lumens/meter^2 at 5550 Å,

$$\text{i.e.,} \ 3.3 \times 10^{-14} \times 4.22 \times 10^{15} \ \text{photons/sec.}$$

$$141 \ \text{photons/sec.}$$

23rd magnitude is therefore equal to 8.8 photons/sec incident upon the telescope aperture. If we compare this with the energy obtainable from the balloon at the telescope aperture, then there is no need to consider the quantum efficiency of the optical system or the detector.

The energy collected from the balloon was

$$6.3\, A_B \times 10^{-4} \ \text{photons/sec.}$$

Therefore for detection by a 200" telescope,

$$A_B \text{ must be } 1.4 \times 10^4.$$

Therefore the diameter must be at least 120 meters. This represents the minimum size of passive balloons that can be tracked optically from Earth.

Let us now consider what information can be gained by tracking such a balloon through the belt.

Taking the mass of the belt as being .001 of that of the Earth (Kuiper) and its boundaries as 2 AU, 3.5 AU and $\pm$ 10° to the ecliptic, one can show that the average density is 0.06 gms/cubic km. If one further assumes that the balloon trajectory through the belt is along the ecliptic, radially outwards from the Sun, i.e., 1.5 AU long, the total mass encountered per square meter of frontal area is

$$(0.06 \times 10^{-6}) \times 1.5 \times (150 \times 10^6) \text{ gms}$$

$$\text{i.e. } 13.5 \text{ gms}$$

Therefore, a balloon of 120 meters diameter would, if the asteroid mass distribution was homogeneous, encounter approximately 11 kg of particles. If we now take into account the orbital velocity of the asteroids, and assign a mean value of 20 km/sec to them, the intercepted mass increases by a factor of 3 or so, taking the balloon velocity at 7 km/sec (approximately correct for a 100 day mission).

The total mass encountered is now 33 kg, and the average relative velocity is 22 km/sec. To evaluate the effect of this on the balloon trajectory, non-destructive transfer of momentum between the particles and balloon has to be assumed.

The mass of a 120 meter balloon can be easily estimated. Assuming a .001" Mylar balloon,

$$\text{Mass} = \pi (120)^2 \times (\frac{2.5}{1000} \times 10^{-2}) \times 1.78 \times 10^6 \text{ gms}$$

$$= 1980 \text{ kg.}$$

The momentum transferred by impinging mass will be 33 x 22 kg km/sec, which should therefore cause a velocity change in the balloon, of 0.36 km/sec, which is certainly large enough to be detected.

SUMMARY

The above calculations indicate that it is possible, with good viewing conditions, to track a 120 meter balloon to 3 AU with the 200" Mt. Palomar telescope. In practice, if several consecutive nights viewing were essential the limiting magnitude may well be 21st or even 20th magnitude, giving a minimum balloon size of 300-1000 meters. In addition, the momentum transfer between the balloon and the hypervelocity particles striking it is not liable to be 100% efficient and the trajectory deflection will therefore be proportionally less. Quite apart from these considerations it is evident that a completely passive balloon probe leads to the inefficient use of available payloads, a 120 meter balloon weighing several thousand pounds. The use of smaller balloons together with a radio beacon would undoubtedly be a more efficient configuration, a 12 meter balloon with a 10 watt beacon for instance would weigh under 200 lbs. Its deflection would be substantially less however, since the majority of its weight would be in the power supplies and not in providing a large surface area.

A further step away from the passive balloons would be to employ a balloon of the type that hardens under the space environment and use its surface as a diaphragm for a conventional micrometeorite counter, telemetering the information back.

APPENDIX II

REQUIRED POWER FOR AN ASTEROID RADAR EXPERIMENT

It was suggested earlier that a radar experiment could be used to determine the population of large particles in the asteroid belt. The power requirements and overall feasibility of such an experiment will now be examined.

Because of the lack of knowledge on the surface features of bodies in the asteroid belt it is proposed for the purposes of this calculation to assume that the radar properties of the asteroids are similar to those of of the moon, i.e., its radar albedo is approximately 0.1, and reflection is non-isotropic with an increase in received power of a factor of two, (theoretical estimates for the moon give a gain of 1 to 6 over isotropic)[21].

The radar equation gives us

$$P_r = \frac{P_t A^2 \rho g a^2}{4\lambda^2 R^4} \quad \text{watts}$$

where

P_r = received power

P_t = transmitted power

A = antenna area

ρ = albedo = 0.1

g = directivity factor = 2

a = radius of target

R = target range

λ = wavelength

If we assume a receiver noise temperature of 100° K and a bandwidth of 1 mc/s to take care of any spectral broadening, then the value of P_r for a signal to noise ratio of 10 db comes to -140 db W. Let us consider an X-band system of 200W peak power (say), with a 1 meter diameter antenna, and calculate its potentialities.

We have, for a frequency of 8 km/c,

P_t = -140 db W

λ^2 = 14.1 x 10^{-4} square meters

A^2 = 0.62 meters^4

ρ = 10^{-1}

Therefore the target will be detected if

$$\frac{200 \times 0.62 \times 0.1}{56.4 \times 10^{-4}} \quad \frac{a^2}{R^4} \quad 10^{-14}$$

i.e., if $a^2/R^4 \quad 4.5 \times 10^{-18}$

i.e., if $a/R^2 \quad 2.1 \times 10^{-9}$

A plot of this relationship for a range of transmitter pulse power is given in Figure A. From this graph it can be seen that an extremely useful experiment can be obtained for very moderate pulse powers. A 1 kw pulsed system for example (which would only consume on average a few watts) could 'see' Icarus at a range of 1500 km, or 10 cm particles at up to 12 km range. Below 10 cm diameter, the particles no longer follow the same

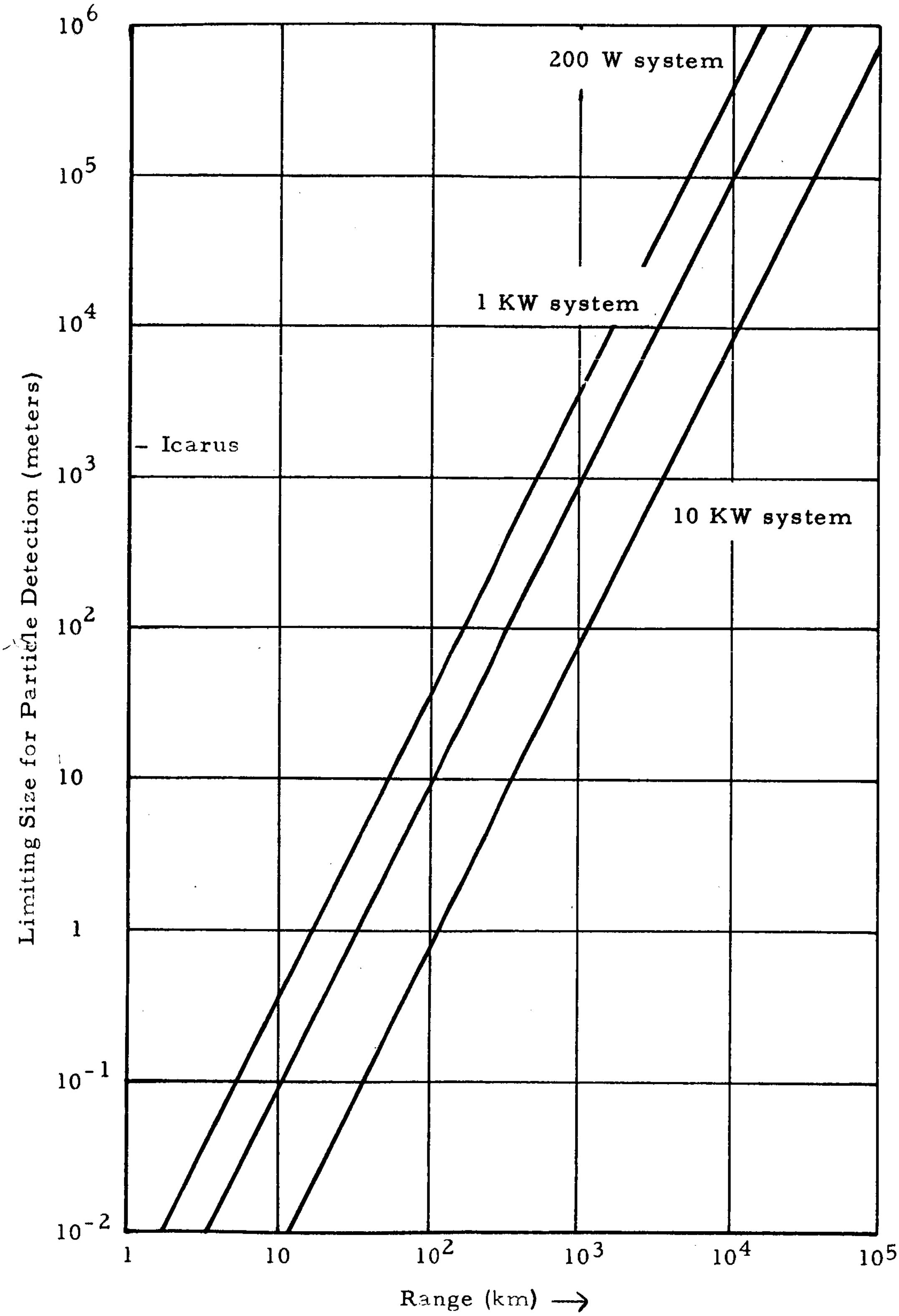

Fig. A DETECTION CAPABILITIES OF AN X-BAND RADAR SYSTEM USING A 1 METER DIAMETER ANTENNA reflection laws, but if they occur with sufficient frequency, i.e., small enough spacing, significant echoes will still be obtained. A table of the capabilities of a radar system using 1000 W pulses is given in Table 3.

There seems to be no reason why this experiment could not alternatively be performed by a laser radar, with a possible saving in weight. A second alternative is simply to scan with a small telescope, but in this case, the determination of the particle size would involve a sophisticated image tube plus a computing capability to

a) separate the asteroids from the stellar background

b) estimate their angular diameter and brightness

Since no range information could be obtained with a single telescope, estimates of the size distribution would rely on the assumption that all asteroids have the same albedo - an assumption which is known to be invalid.

It is concluded that the most efficient, and economical method of studhing the large particle distribution in the belt would be by a radar experiment such as has been described. The use of optical frequencies (i.e. lasers) would extend the range of observable particles down to the micron region[22].

APPENDIX III

TERMINAL AND MID-COURSE GUIDANCE

Mid-Course Guidance

A digital computer program has been developed to study the heliocentric trajectory sensitivity to injection errors, and the resulting mid-course ΔV requirements. The analysis is based on linear perturbations about a precomputed reference trajectory, and statistical covariance techniques. The four target parameters chosen to be investigated are the two positional miss components (Δb_T and Δb_R), the time-of-flight error (ΔTF), and the approach velocity magnitude error (ΔVHP) existing at the point where the perturbed approach trajectory to the target asteroid intersects a hypothetical target plane. R and T are two mutually perpendicular axes lying in the target plane. Their particular orientation is of no importance for guidance error computation. Following accepted procedure, the target plane moves along with the asteroid in its orbit and is defined to be normal to the reference asymptotic approach direction, $\overline{S}$. Two types of mid-course velocity corrections are considered. These are (1) terminal position plus time-of-flight correction (FTA), and (2) correction of terminal position only with minimum ΔV (VTA). The latter type of correction is included to characterize those missions that may allow variable time-of-arrival guidance. In neither case is the approach velocity explicitly controlled.

Results are described here for a 100 day Earth-Eros trip having a launch date 1/20/68. The reference trajectory is characterized by a hyperbolic excess velocity at launch of 7.8 km/sec, an inclination of 10.8°, a heliocentric transfer angle of 91.2°, and a hyperbolic excess velocity at arrival of 3.76 km/sec. The point should be made that this trajectory is not necessarily typical or desirable, but is used only as a representative example. Guidance results for a range of asteroid missions were shown in earlier sections of this report.

The position errors at injection are assumed zero, and the heliocentric velocity errors (equivalent to launch hyperbolic excess velocity errors) are assumed to be 10 meters/sec RMS in each component, uncorrelated. These error magnitudes are equivalent to propagations of 4-5 meters/sec cut-off errors. The resulting target errors (RMS) are

$$\Delta b_T = 73,300 \text{ km}$$

$$\Delta b_R = 53,600 \text{ km}$$

$$\Delta TF = 219 \text{ min.}$$

$$\Delta VHP = 18.4 \text{ m/sec.}$$

Assuming a single mid-course correction, Figure B shows the velocity increment required as a function of the time of correction. The expected result that the ΔV_c cost of guidance increases with time is in evidence. The cost of the FTA correction is 19 m/sec at 10 days or 30.6 m/sec at 40 days. Note that the minimum ΔV_c correction offers a saving of several meters per second if variable time-of-arrival guidance is allowable.

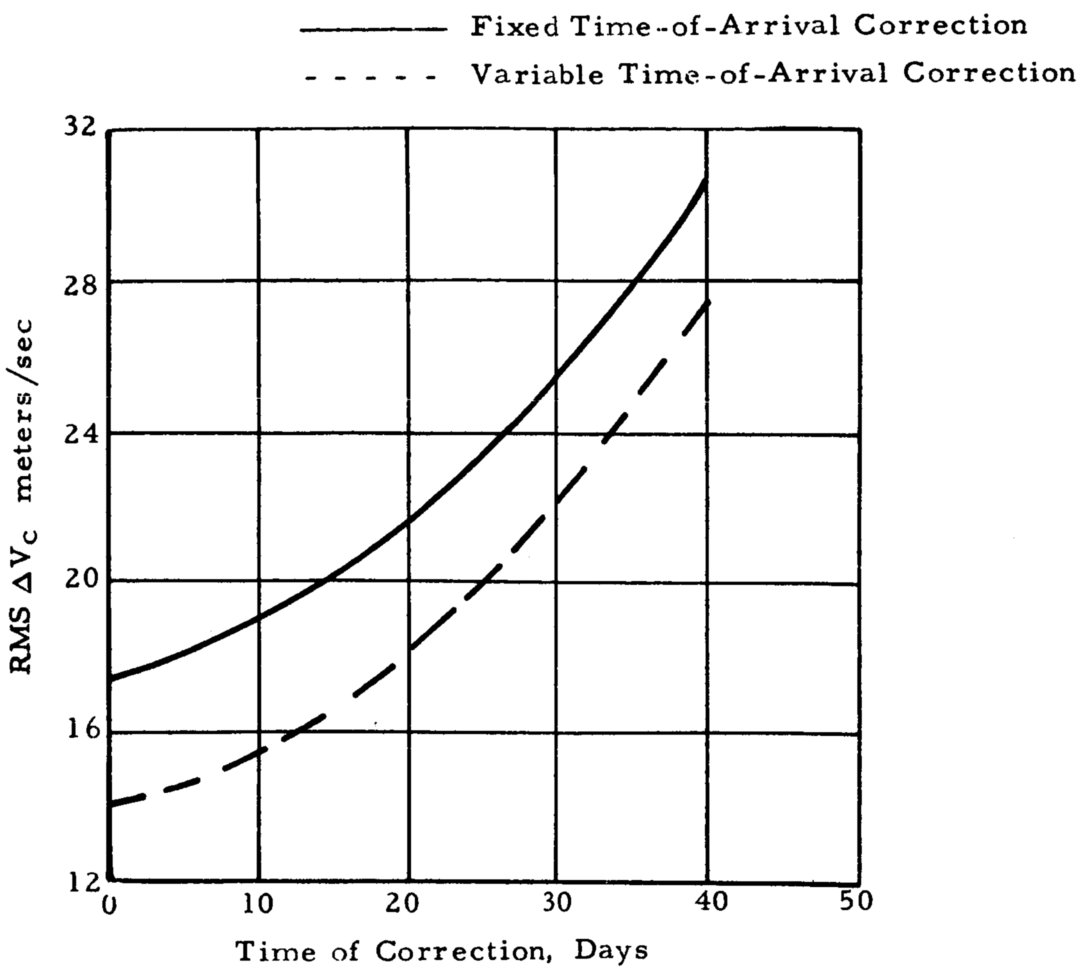

Fig. B MID-COURSE VELOCITY REQUIREMENT (SINGLE CORRECTION) 100 DAY EARTH-EROS TRAJECTORY, LAUNCH 1/20/68

The approach velocity error remaining after the correction is shown in Figure C. This error is largest for the minimum ΔV_c correction, which is to be expected inasmuch as the approach velocity and time-of-flight errors are fairly well correlated. One also notes that the velocity error is significantly reduced from its initial value of 18.4 m/sec even though this variable is not explicitly controlled. The time-of-flight error remaining after the minimum ΔV_c correction is similar in its characteristics to the velocity error, and varies between 190 and 201 minutes.

Terminal Guidance

Figure D illustrates the geometry of terminal guidance maneuvers. The spacecraft approaches the target with a velocity VHP, which remains essentially constant due to the negligible gravitational field of the asteroid. The miss distance b is the residual mid-course guidance position error. Correction of this error with a minimum velocity impulse is accomplished by applying ΔV_c normal to the line-of-sight (LOS). The minimum impulse is given by the relation

$$\Delta V_c = \frac{VHP \cdot b}{r}$$

The ratio $\Delta V_c/VHP$ is plotted in Figure E as a function of the range at which the impulse is applied and the miss distance. For example, a 3000 km error corrected at a range of 100,000 km would require a velocity increment equal to 3 per cent of the approach velocity. A second velocity increment equal to VHP would then be applied at close range to reduce the relative motion to zero. Such a two-impulse terminal maneuver requires a total velocity increment of

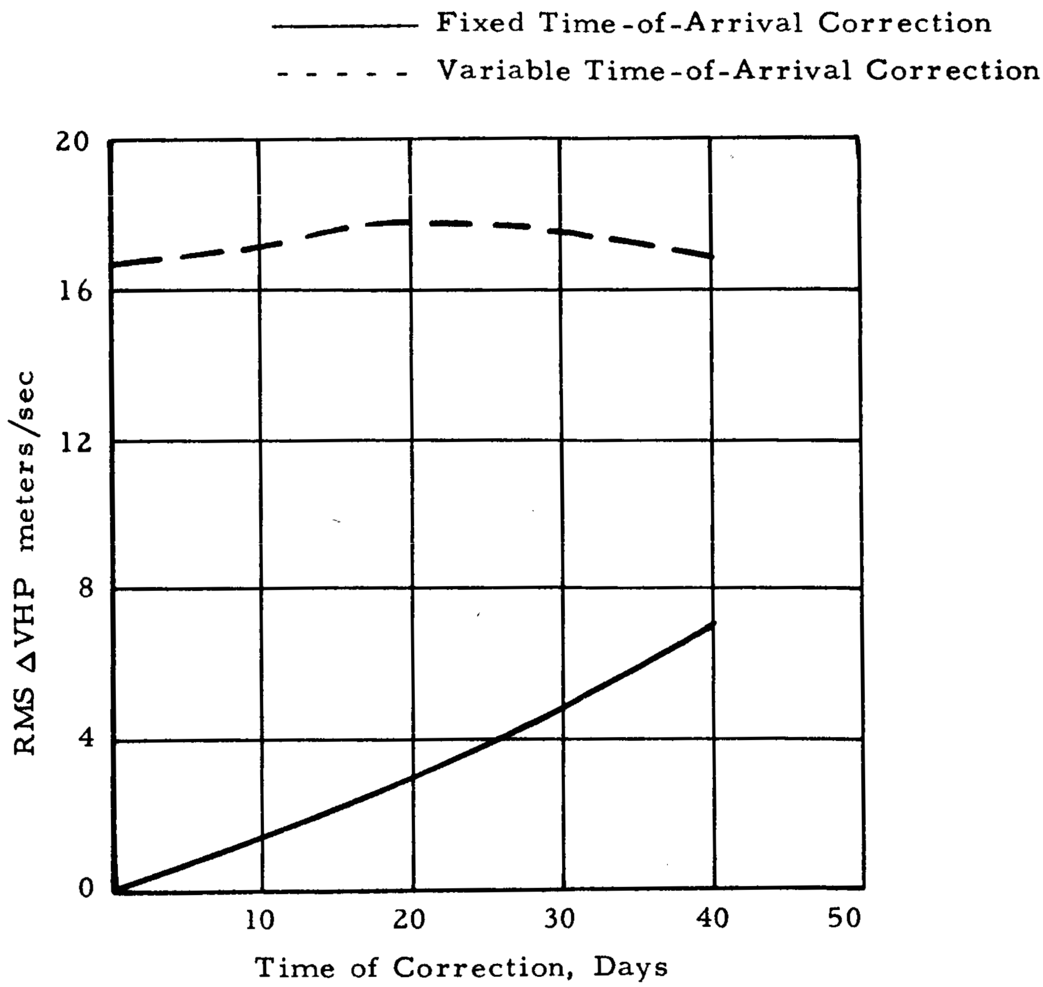

Fig. C APPROACH VELOCITY ERROR REMAINING AFTER CORRECTION - 100 DAY EARTH-EROS TRAJECTORY, LAUNCH 1/20/68

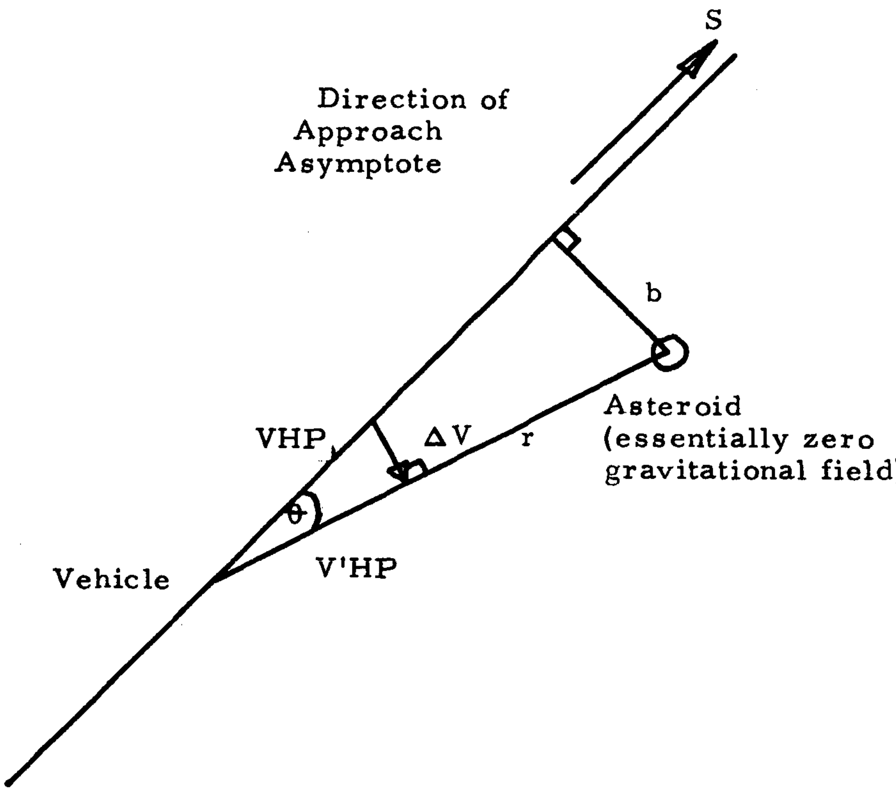

Fig. D TERMINAL GUIDANCE GEOMETRY

$$1 \leq \frac{\Delta V_c}{VHP} + \quad 1 - \left(\frac{\Delta V_c}{VHP}\right)^2 \leq \sqrt{2}$$

Hence, a maximum velocity penalty of 41 per cent results if the miss correction is made at the condition $b/r = 1/\sqrt{2}$. Obviously, this type of terminal maneuver is not necessarily optimum in an overall sense. Other guidance policies should be examined. For example, if the initial miss distance were not too large, say within 10, 000 km, one might defer action until the point of closest approach is reached, at which time a velocity increment equal in magnitude and oppositely directed to VHP would be applied. A second closing impulse would then be applied, followed by a third impulse of equal magnitude applied at close range. If the time required for closing were not critical, the total velocity cost would be, in the limit, equal to VHP.

The basic navigational variables of interest for terminal guidance are easily derived from the geometry. The following relations obtain, in two dimensions

$$b = r \sin \theta = \frac{r^2 \dot{\theta}}{VHP} = \frac{VHP \sin^2 \theta}{\dot{\theta}}$$

where θ is the LOS angle relative to the approach direction (fixed in inertial space) and $\dot{\theta}$ is the LOS rate. Mid-course guidance analysis has indicated that VHP is not exceptionally sensitive to perturbations. Hence, rather than attempting to measure VHP, it may be sufficient to use its predicted value in the computation of b. The range r is very useful navigational information, however, it is not so readily obtained. Active radar systems normally require very high power at long range and hence high weight. Apparent size

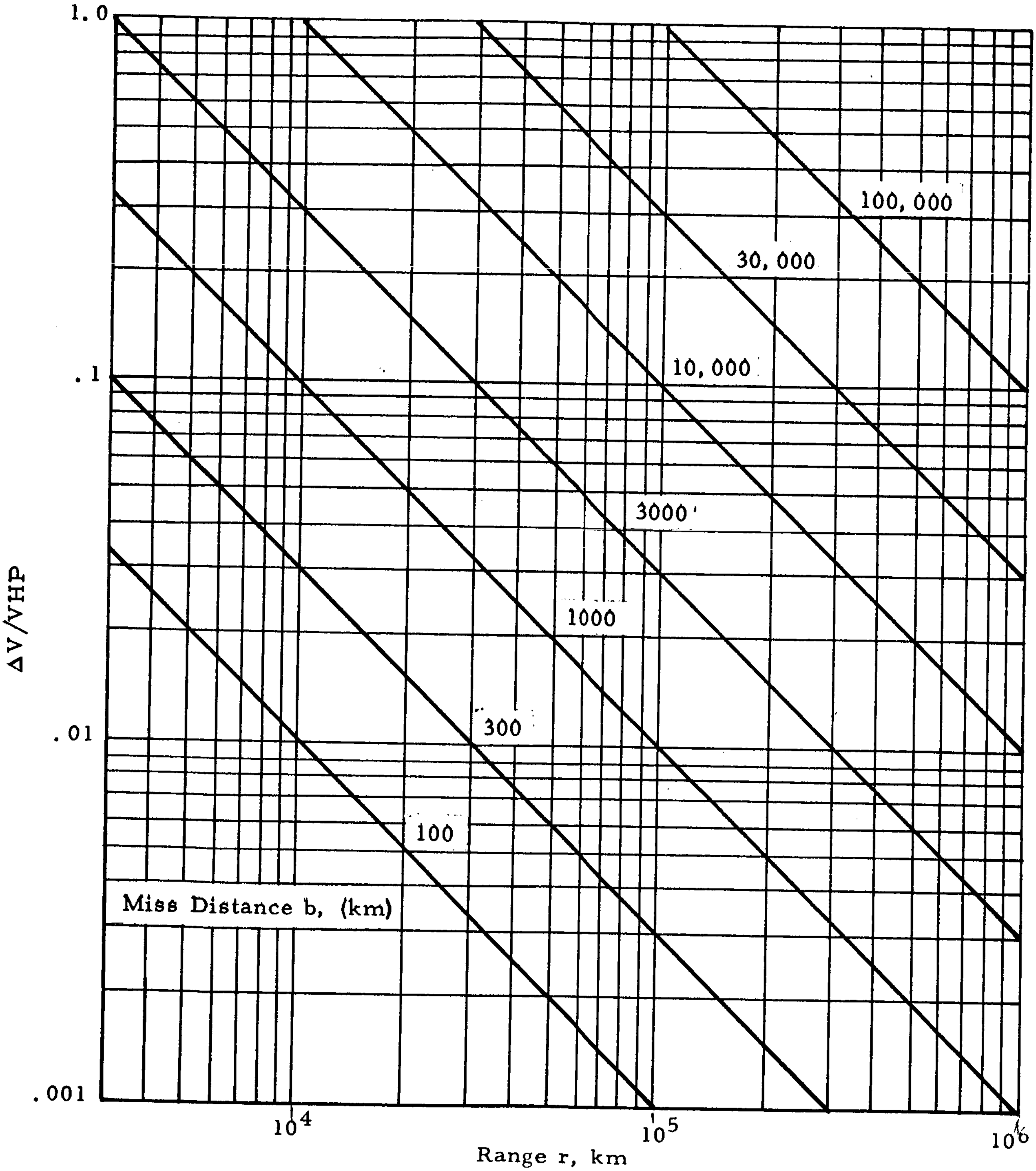

Fig. E TERMINAL CORRECTION REQUIREMENTS

measurements of an asteroid using optical techniques is made difficult by its small size and irregular shape. This leaves the LOS angle and its rate of change as logical candidates for measurement. Passive radar, optical, or infrared trackers, either gyro-stabilized or having rate gyros mounted on a body-fixed platform, are possible choices for determining this information. Another possibility would be an optical/television system which would view the target asteroid against a known star background.

Figure F shows a plot of the LOS rate as a function of range and miss distance for an approach velocity of 10 km/sec. This figure indicates the relatively small angular rates that are involved. For example, if b is 10,000 km θ varies from 10^{-5} to 10^{-3} radians/sec as r decreases from 100,000 km. Since θ is directly proportional to b and VHP, even smaller rates may be in effect. Rate information could be derived from differentiating networks, however, noise is apt to be a very difficult problem to overcome. It is evident that this area of LOS and LOS rate measurement techniques needs a much closer examination.

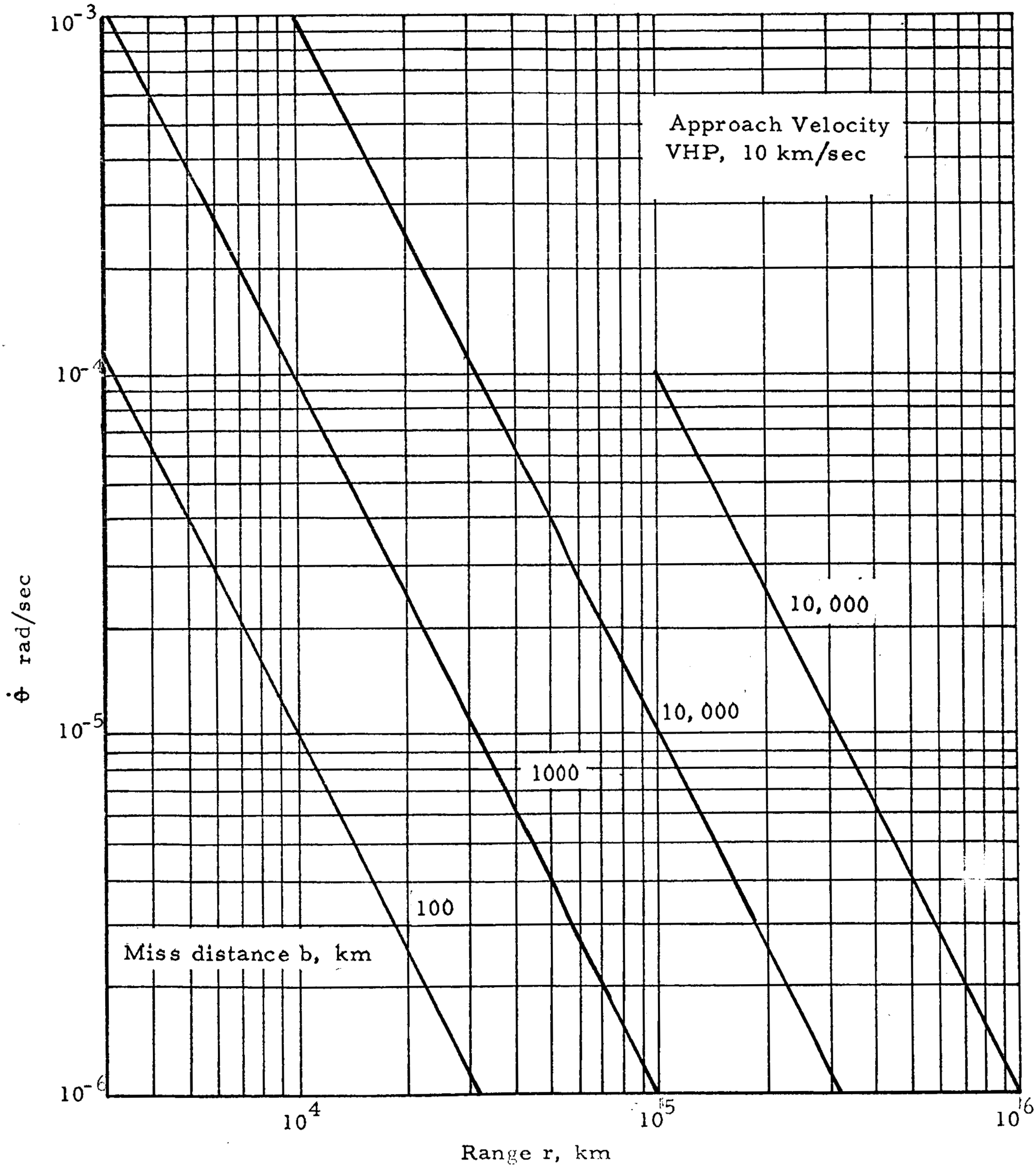

Fig. F LOS RATE - TERMINAL PHASE